MODELING OF SEDIMENT YIELD USING SOIL AND WATER ASSESSMENT TOOL: THE CASE STUDY OF HUMBO WEYNE DAM, SOMALILAND

RIDWAN SAED FARAH

A THESIS SUBMITTED TO THE DEPARTMENT OF WATER RESOURCES ENGINEERING, COLLEGE OF CIVIL ENGINEERING AND ARCHITECTURE

PRESENTED IN PARTIAL FULFILLMENT OF THE REQUIREMENTS FOR THE DEGREE OF MASTER'S IN WATER RESOURCES ENGINEERING (SPECIALIZATION IN HYDRAULIC ENGINEERING)

SCHOOL OF GRADUATE STUDIES
ADAMA SCIENCE AND TECHNOLOGY UNIVERSITY

January, 2026
Adama, Ethiopia

MODELING OF SEDIMENT YIELD USING SOIL AND WATER ASSESSMENT TOOL: THE CASE STUDY OF HUMBO WEYNE DAM, SOMALILAND

RIDWAN SAED FARAH

ADVISOR: DR. ZELALEM BIRU (Ph.D.)

A THESIS SUBMITTED TO THE DEPARTMENT OF WATER RESOURCES ENGINEERING, COLLEGE OF CIVIL ENGINEERING AND ARCHITECTURE

PRESENTED IN PARTIAL FULFILLMENT OF THE REQUIREMENTS FOR THE DEGREE OF MASTER'S IN WATER RESOURCES ENGINEERING (SPECIALIZATION IN HYDRAULIC ENGINEERING)

SCHOOL OF GRADUATE STUDIES
ADAMA SCIENCE AND TECHNOLOGY UNIVERSITY

January, 2026
Adama, Ethiopia

DECLARATION

I declare that this Master's Thesis entitled **Modeling of Sediment Yield Using Soil and Water Assessment Tool: The Case Study of Humbo Weyne Dam, Somaliland** is my own work. It has not been submitted for the award of any academic degree, diploma, or certificate in any other university. All sources of materials that are used for this thesis have been duly acknowledged through citation.

Ridwan Saed _____ _____

Name of student Signature Date

RECOMMENDATION

I, the advisor of this thesis, hereby certify that I have read the revised version of the thesis entitled **Modeling of Sediment Yield Using Soil and Water Assessment Tool Model: The Case Study of Humbo Weyne Dam, Somaliland** prepared under my guidance by Ridwan Saed submitted in partial fulfillment of the requirements for the degree of Master's in Water Resources Engineering (Specialization in Hydraulics Engineering).

Therefore, I recommend the submission of a revised version of the thesis to the department following the applicable procedures.

_____	_____	_____
Advisor	Signature	Date

APPROVAL PAGE

I, the advisor of the thesis entitled **Modeling of Sediment Yield Using Soil and Water Assessment Tool Model: The Case Study of Humbo Weyne Dam, Somaliland** and developed by **Ridwan Saed**, hereby certify that the recommendations and suggestions made by the board of examiners are appropriately incorporated into the final version of the thesis.

Advisor	Signature	Date

We, the undersigned, members of the Board of Examiners of the Thesis, by **Ridwan Saed**. Have read and evaluated the thesis entitled **Modeling of Sediment Yield Using Soil and Water Assessment Tool Model: The Case Study of Humbo Weyne Dam, Somaliland** and examined the candidate during open defense. This is, therefore, to certify that the thesis is accepted for partial fulfillment of the requirements of the degree of Master of Science in the Department of Water Resources Engineering, College of Civil Engineering and Architecture.

Chairperson	Signature	Date
Internal Examiner	Signature	Date
External Examiner	Signature	Date

Final approval and acceptance of the thesis is contingent upon submission of its final copy to the Office of Postgraduate Studies (OPGS) through the Department Graduate Council (DGC) and School Graduate Committee (SGC).

Department Head	Signature	Date
School Dean	Signature	Date
Office of Postgraduate Studies, Dean	Signature	Date

ACKNOWLEDGEMENT

All praise and gratitude are due to Allah, the Most Gracious, the Most Merciful, for bestowing upon me the strength, knowledge, and perseverance to bring this research to fruition.

I extend my deepest and most sincere appreciation to my supervisor, Dr. Zelalem Biru Gonfa. His invaluable guidance, critical insights, and unwavering support have been the cornerstone of this thesis. His mentorship has not only shaped this research but has also profoundly contributed to my academic and professional development.

I would like to extend my gratitude to the Ethiopian Meteorological Institute (EMI) and the Ministry of Water and Energy of Ethiopia for graciously providing the essential meteorological and hydrological data for the Gode catchment that formed the basis of the regionalization analysis. I also acknowledge FAO-SWALIM (Somalia Water and Land Information Management) for their valuable weather data, which was instrumental in driving the hydrological simulation of the study area.

I am eternally indebted to my beloved family for their unconditional love, endless encouragement, and steadfast belief in me. Their sacrifices and prayers have been a constant source of motivation throughout this challenging journey.

Finally, I acknowledge my own determination and resilience in navigating the complexities of this research. The dedication and hard work invested have been a significant personal and scholarly achievement.

TABLE OF CONTENTS

LIST OF TABLES

LIST OF FIGURES

LIST OF ABBREVIATIONS AND ACRONYMS

95PPU	95% Prediction Uncertainty
CHIRPS	Climate Hazards Group Infrared Precipitation with Station Data
CN	Curve Number
CNI	Curve Number at Dry Condition
CNII	Curve Numberat Normal or Average Condition
CNIII	Curve Number at Wet Condition
DEM	Digital Elevation Model
DGC	Department Graduate Council
DSMW	Digital Soil Map of the World
DSOLMap	Digital Soil Property Map
EMI	Ethiopian Meteorological Institute
ENSO	El Niño-Southern Oscillation
ERA5	European Centre for Medium-Range Weather Forecasts Reanalysis V5
ET	Evapotranspiration
ETB	Ethiopian Birr
FAO	Food and Agriculture Organization
GCS	Geographic Coordinate System
GHMs	Global Hydrological Models
GIS	Geographic Information System
HRU	Hydrologic Response Unit
LSU	Landscape Unit
LULC	Land Use/Land Cover
MoWIE	Ministry Of Water, Irrigation and Electricity
MUSLE	Modified Universal Soil Loss Equation
MWSWAT	MapWindow SWAT
NASA	National Aeronautics and Space Administration.
NSE	Nash-Sutcliffe Efficiency
OPGS	Office of Postgraduate Studies
PBIAS	Percent Bias
R^2	Coefficient of Determination
RFR	Random Forest Regression
RMSE	Root Mean Square Error

RSR	RMSE-observations Standard Deviation Ratio
RUSLE	Revised universal soil loss equation
SCS	Soil Conservation Service
SEDEM	Sediment Delivery Model
SGC	School Graduate Committee
SRTM	Shuttle Radar Topography Mission
SUFI2	Sequential Uncertainty Fitting version 2
SWALIM	Somalia Water and Land Information Management
SWAT	Soil and Water Assessment Tool
SWAT_CUP	SWAT Calibration and Uncertainty Programs
TOA	Top of Atmosphere
USGS	United States Geological Survey
USLE	universal soil loss equation
UTM	Universal Transverse Mercator
WaTEM	Water and Tillage Erosion Model
WGS	World Geodetic System
WoSIS	World Soil Information Service

ABSTARCT

Reservoir sedimentation presents a critical threat to water security in the semi-arid Horn of Africa, where infrastructure lifespan is often compromised by extreme soil erosion. The Humbo Weyne Dam, a vital water source for Hargeisa, Somaliland, is currently facing severe dysfunction due to rapid siltation, which has drastically reduced its 500,000 m³ design capacity. This study aimed to quantify the annual sediment yield entering the reservoir and identify critical erosion hotspots using the Soil and Water Assessment Tool (SWAT) model. Due to the absence of local hydrological data, a spatial proximity regionalization approach was employed, transferring calibrated parameters from the spatially proximate gauged Gode catchment (Wabi Shebelle basin) to the ungauged Humbo Weyne watershed. The model was set up using high-resolution 30m SRTM DEM, FAO soil maps, and Copernicus Land Use data, driven by bias-corrected CHIRPS satellite rainfall and ERA5 climate reanalysis products. The model performance on the donor catchment was reliable, achieving Nash-Sutcliffe Efficiencies (NSE) of 0.86 for streamflow and 0.81 for sediment yield. For the ungauged Humbo Weyne catchment, the SWAT+ model was utilized to simulate sediment dynamics at the Landscape Unit (LSU) level. The results indicate an average annual sediment yield of 4.9 t/ha/yr, translating to a total influx of approximately 660,000 tons of sediment per year a volume that explains the rapid loss of reservoir storage. Spatial analysis revealed that erosion is not uniform; critical hotspots in the northeastern escarpment, covering only 19.8% of the area, generate severe yields exceeding 35 t/ha/yr. These findings provide the first quantitative evidence to guide targeted soil conservation measures, such as hillside terracing and check dams, which are essential to rehabilitate the existing structure and safeguard future water infrastructure development at this strategic site.

Keywords: Humbo Weyne Dam, Regionalization, Sediment Yield, Somaliland, Spatial Variability, SWAT Model.

CHAPTER ONE: INTRODUCTION

1.1 Background of the study

Sedimentation, the process of soil particles being transported and deposited in water bodies, presents a critical threat to global water resources, impacting economic, social, and environmental dimensions. It diminishes reservoir storage capacity, degrades water quality, and disrupts aquatic ecosystems (Amini, 2018; Gurmu et al., 2022). This issue is amplified by unsustainable land use, deforestation, and climate change, particularly in vulnerable regions like sub-Saharan Africa (Amini, 2018; Gurmu et al., 2022). Recent research indicates a global surge in sedimentation rates, largely attributed to land use changes (Gonzalez Rodriguez et al., 2023), with climate change projections further escalating the problem, as exemplified by the Xin'anjiang Reservoir Basin where sediment yield is predicted to increase by 41.03-54.88% by 2100 (Li et al., 2022). This global trend is underscored by a comprehensive assessment of 47,403 large dams, projecting a 26% global storage loss by 2050 (Perera et al., 2022). The economic consequences of sedimentation include diminished reservoir capacity, exemplified by a 39% reduction in the Chimhanda Dam, Zimbabwe (Tundu et al., 2018), damage to infrastructure like dam outlets and water intakes (Randle et al., 2013), and declines in economic activity, as seen in the Asahan River's declining port activities (Bakti et al., 2024). Socially, sedimentation contributes to community displacement due to increased flood risks (Bakti et al., 2024) and exacerbates water scarcity by reducing water quality and quantity, thus increasing purification costs (Tundu et al., 2018). Environmentally, sedimentation leads to biodiversity loss due to sediment-bound contaminants and habitat degradation (Wharton et al., 2017), and alters downstream river morphology, impacting aquatic life and ecosystem services (Shrivastava & Rai, 2023).

Given the widespread impacts of sedimentation, effective management strategies are crucial. Integrating advanced modeling techniques can provide valuable insights for sustainable water resource management, especially under changing climatic conditions (Ayele et al., 2021; Do et al., 2022). One such technique is sedimentation modeling, particularly crucial in semi-arid environments around dams where reservoir capacity and lifespan are directly affected. The Soil and Water Assessment Tool (SWAT), a semi-distributed, continuous, physical-based model, has become a prominent tool for predicting sediment yield and hydrological processes due to its efficiency and reported accuracy (J. G. Arnold et al., 2012). Numerous studies demonstrate SWAT's applicability in various semi-arid watersheds. For instance, the SWAT has been successfully applied to the Merguellil watershed in Tunisia

(Ines Gharnouki et al., 2024), while in the Tata basin, Morocco, the SWAT was used to estimate sediment production rates (Echogdali et al., 2022). Further applications include reservoir management, as seen in the Koyna basin, India, where SWAT was employed to predict sediment load, identifying sub-basins with high erosion rates that require immediate conservation efforts (Sabale et al., 2023). And the Singda Dam in Manipur, India, where the SWAT model was utilized alongside Remote Sensing and GIS techniques to assess sedimentation, achieving a high coefficient of determination for sediment loss, indicating the model's reliability in similar geological settings (Sophiya & Updhayaya, 2023).

This global challenge is particularly acute in Africa, where sedimentation significantly impacts water supply, irrigation, and hydropower generation. Understanding sediment yield is essential for assessing reservoir longevity, as exemplified by studies on the Angereb reservoir in Ethiopia (S. M. Tessema, 2011). Land-use changes, such as the expansion of farmland, often exacerbate sedimentation, as seen in the Vea reservoir study (Atulley et al., 2022). This issue is particularly pronounced in East Africa, especially the Horn of Africa, where climatic factors and land-use practices create unique sedimentation challenges. In addition, the Horn of Africa experiences highly variable rainfall patterns, with increasing drought frequency by a rise of 5-10% in severe droughts from 1986 to 2020, according to Alasow et al., (2024), and intense rainfall events, both of which exacerbate sedimentation. This variability is further complicated by the influence of the El Niño-Southern Oscillation (ENSO), which leads to alternating periods of flooding and drought, disrupting sediment dynamics (Mologni et al., 2024). Exacerbating these climatic factors are unsustainable land-use practices. Overgrazing contributes to soil degradation and increased sediment runoff (Alasow et al., 2024), while deforestation for agriculture reduces vegetation cover, further increasing erosion and sedimentation in rivers and lakes (Baxter et al., 2023).

This regional crisis of accelerated reservoir sedimentation is acutely manifested at the Humbo Weyne Dam in Somaliland. Intended to alleviate critical water scarcity in the capital city of Hargeisa, the dam was designed with a storage capacity of 500,000 m^3 (Daud, 2022), However, despite being situated on a robust basalt foundation that could potentially support a hydraulic head of 40-60m (Somaliland Channel, 2017), the current infrastructure built with a head of only 15m has critically underperformed.

Reports indicate that the dam's effective capacity was drastically reduced by rapid siltation even before it reached full operational status (Staff, 2018). The construction manager, Wassim Haroun, confirmed that high sediment loads from the upstream catchment have

compromised the reservoir's lifespan (Staff, 2018),Furthermore, the Hargeisa Water Agency has previously flagged the project's underperformance as a significant failure in meeting the city's water demands (SAAB TV, 2018), This rapid loss of storage capacity highlights a complex interplay of environmental factors including deforestation, overgrazing, and recurring droughts which have accelerated land degradation and sediment transport in the Humbo Weyne wadi (Abdulkadir, 2017).

Given that the current dam captures a mere fraction (estimated at 3%) of the annual streamflow (Somaliland Channel, 2017), understanding the sediment dynamics is an engineering necessity. It is vital not only for the rehabilitation of the existing structure but to ensure that this strategic site with its high hydraulic potential is not permanently degraded by unchecked erosion. To address this challenge, this research investigated the drivers of sedimentation at the Humbo Weyne Dam using the SWAT model. Due to the limited observed sediment data at the site, model calibration leveraged the spatial proximity regionalization method. By quantifying sediment yield and identifying the most erosion-prone sub-basins, this study aims to inform sustainable water resource management strategies, ensuring the long-term effectiveness of the Humbo Weyne Dam and guiding future water infrastructure development in Somaliland. Ultimately, this research addresses the pressing issue of water security in the region, preventing the potential economic and social consequences of continued water scarcity.

1.2 Problem Statement

The Humbo Weyne Dam, a vital infrastructure project designed to secure water for Hargeisa, is currently in a critical state of dysfunction. The dam is losing its designed storage capacity of 500,000 m^3 at an alarming rate due to excessive sediment inflow, rendering it unable to fulfill its primary objective of alleviating water scarcity z.

Despite this urgent failure, there is a complete absence of quantitative data regarding the catchment's erosion dynamics. The watershed is entirely ungauged, meaning no historical records of streamflow or sediment concentration exist. This data vacuum has forced engineers and decision-makers to rely on assumptions rather than empirical evidence, preventing the design of effective dead storage zones or targeted soil conservation measures.

Without a scientific assessment of where the sediment is coming from and how much is entering the reservoir annually, any attempt to rehabilitate the existing dam or construct new ones in the region risks repeating the same costly failure. This study addresses this gap by

using the SWAT model and regionalization techniques to quantify the sediment yield and identify the specific erosion hotspots threatening the dam's sustainability.

1.3 Research questions

1. How accurately does the SWAT model simulate sediment yield within the gauged watershed?
2. What is the annual rate of sediment influx into the Humbo-Wayne reservoir?
3. Which sub-basins within the Humbo-Wayne watershed are most susceptible to erosion?

1.4 The significance of this study

The Humbo Weyne Dam, intended as a vital water source for Hargeisa, Somaliland, is currently compromised by rapid sedimentation, severely affecting the region's water security. This study is significant because it provides the first quantitative assessment of the sediment dynamics threatening this infrastructure. By successfully applying the SWAT model with regionalization techniques, this research established a specific annual sediment yield of 4.9 t/ha/yr and a total annual influx of approximately 660,000 tons.

This information is critical for three key reasons:

1. **Targeted Intervention:** It identified specific high-risk zones, such as the northeastern escarpment, allowing decision-makers to prioritize limited financial resources for soil conservation where they are most needed, rather than applying generic measures across the entire basin.
2. **Engineering Design:** The calculated sediment influx provides essential data for determining the necessary dead storage capacity for any future rehabilitation of the dam or construction of new reservoirs in the region, preventing the design failures of the past.
3. **Methodological Proof:** The study demonstrated the viability of using spatial proximity regionalization and global satellite datasets (CHIRPS/ERA5) to model ungauged catchments in Somaliland. This offers a proven methodological framework that researchers and engineers can replicate to assess water resources in other data-scarce regions of the Horn of Africa.

1.5 Objectives

1.6 General objectives

The general objective of this Thesis is to assess the current sedimentation status of the Humbo Weyne Dam and predict future sedimentation rates for the region, ensuring the long-term water security of Hargeisa.

1.7 Specific objectives

i. To evaluate the performance of the SWAT model for estimating sediment yield within the Gauged catchment.
ii. To quantify the yearly rate of sediment influx into the reservoir.
iii. To determine the most susceptible sub-basin to erosion and visualize the spatial pattern of sediment transport to the reservoir.

1.8 Scope of the study

This study focused on the Humbo Weyne watershed, encompassing all upstream areas contributing water and sediment to the Humbo Weyne reservoir. The primary tool used for simulating hydrological processes and sediment transport was the Soil and Water Assessment Tool (SWAT) model. Due to the absence of local gauging stations, the study employed regionalization techniques based on spatial proximity, utilizing the spatially proximate gauged Gode catchment (Wabi Shebelle basin) as a donor for parameter estimation.

Data collection and analysis included the use of 30m SRTM Digital Elevation Models (DEM), FAO soil maps, Copernicus Land Use/Land Cover data, and bias-corrected CHIRPS satellite rainfall and ERA5 reanalysis climate data. The study modeled outputs to characterize and quantify sediment yield within the watershed, estimated the yearly sediment influx into the reservoir, and successfully identified and mapped critical sediment source areas. While the study did not delve into simulating specific future management scenarios, the results provide a quantitative baseline and specific identification of erosion hotspots (particularly the northeastern escarpment) to guide future engineering and conservation strategies.

CHAPTER TWO: LITERATURE REVIEW

2.1 Soil Erosion and Sedimentation

Soil erosion and sedimentation are interconnected environmental processes with significant implications for agriculture, water resources, and ecosystem health. Erosion involves the detachment of soil particles by forces like raindrop impact, their subsequent transport via surface runoff, and eventual deposition (Foster & Meyer, 1977; Shahin, 2007). These processes can be categorized into natural erosion, which occurs due to climatic and geological factors, and accelerated erosion, which is primarily driven by human activities such as deforestation, improper agricultural techniques, and urbanization (Adnan et al., 2021; Mikos, 2004). Understanding the complex interplay of factors influencing erosion, including climate, soil type, topography, and vegetation cover, is essential for developing effective land management and conservation strategies(Meyer, 1986).

In semi-arid regions like the Horn of Africa, erosion is driven by several interrelated factors. Intense, short-duration rainfall on dry, poorly vegetated soils leads to rapid surface runoff, which can dislodge large quantities of soil and result in flash floods (Megnounif et al., 2007). The erosive potential is heightened where vegetation cover is minimal, making soils more susceptible (Koppa et al., 2022). Compounding this issue are prolonged droughts, which degrade vegetation cover and leave soils exposed. The Horn of Africa has experienced increasing drought frequency, which correlates with significant soil erosion events and a loss of soil structure (Han et al., 2022; Muktadir et al., 2022). These climatic pressures are exacerbated by land use practices such as overgrazing, which compacts the soil, reduces its ability to absorb water, and increases surface runoff(Muktadir et al., 2022). Furthermore, climatic phenomena like the El Niño-Southern Oscillation (ENSO) contribute to cycles of extreme drought and flooding, leading to significant and unpredictable erosion events (Han et al., 2022; Koppa et al., 2022).

While erosion has numerous detrimental effects, the most critical for water infrastructure is reservoir sedimentation. This single issue poses a significant global threat to water storage, with projections indicating a 26% loss in global reservoir capacity by 2050 due to sediment accumulation (Perera et al., 2022). This crisis is particularly acute in the Horn of Africa. For instance, studies in neighboring Ethiopia have documented alarming sedimentation rates, with the Angereb reservoir experiencing a 62.28% reduction in storage capacity over 16 years (Y. M. Tessema et al., 2024), and the Adebra Night Storage Reservoir losing 24.8% of its capacity in just eight years (Mekonnen et al., 2022). These figures highlight the urgent

need for effective sediment management strategies to preserve the lifespan of vital water infrastructure.

This regional crisis of accelerated reservoir sedimentation, driven by a combination of climatic pressures and land use practices, is acutely manifested at the Humbo Weyne Dam. As a vital water source for Hargeisa, Somaliland, the viability of this dam is directly threatened by these processes, underscoring the critical importance of understanding and modeling sediment yield in its catchment.

2.2 Reservoir Sedimentation: Global and Regional Perspectives

Reservoir sedimentation presents a significant global challenge, impacting water storage capacity and ecological balance. The projected decline in global reservoir storage capacity from 6,316 billion cubic meters to 4,665 billion cubic meters by 2050 represents a substantial loss, equivalent to the annual water use of several major countries (Jaiswal et al., 2024). This decline is exacerbated by global changes, including climate variability and land use alterations, which necessitate the development and implementation of effective management strategies. Increased sedimentation rates are linked to altered hydrological conditions resulting from climate change, leading to reduced sediment trapping efficiency within reservoirs and increased flood risks downstream (Haun et al., 2024; Mouris et al., 2023).

Reservoir sedimentation poses significant challenges in the Horn of Africa, impacting water supply, hydropower generation, and irrigation. The region's unique climatic and geographical conditions exacerbate these issues, leading to substantial storage loss in reservoirs. For instance, studies indicate that the Angereb reservoir has experienced a 62.28% reduction in storage capacity over 16 years, with an average annual sedimentation rate of 3.9% (Y. M. Tessema et al., 2024). This loss translates to significant economic consequences, as the global impact of sedimentation is estimated to be between US$10 billion and US$20 billion annually, affecting infrastructure and flood management (Annandale, 2005). Modeling approaches, such as the WASA-SED model, offer valuable tools for simulating sediment transport and retention, providing insights into sustainable land use and reservoir management (Mueller et al., 2010). Case studies in Ethiopia, including the Angereb Reservoir, which saw a sediment deposition of 2.18 Mm^3 between 2007 and 2022 (Y. M. Tessema et al., 2024), and the Adebra Night Storage Reservoir, which lost 24.8% of its capacity in just eight years (Mekonnen et al., 2022), highlight the urgent need for improved soil conservation practices and effective sediment management strategies. While the challenges are substantial, they also present opportunities for innovative management

practices and community engagement in sustainable land use, potentially enhancing reservoir longevity and ecosystem health.

Effective management of reservoir sedimentation relies heavily on accurate monitoring and assessment techniques. Various sediment detection methods, including topographic differencing and sub-bottom profiling, provide essential data for assessing sediment accumulation patterns and informing management decisions (Hilgert et al., 2023).

2.3 Overview of Hydrological Models

A model, whether physical, conceptual, or mathematical, serves as a simplified representation of a phenomenon to facilitate understanding and informed decision-making across diverse fields, especially in science and engineering. Models are crucial for explaining and predicting the behavior of real-world systems, guiding both research endeavors and practical applications. They achieve this by abstracting complex phenomena into more manageable forms, allowing for focused analysis and interpretation. The purpose of a model can vary depending on the specific application, including explaining observed phenomena, controlling system behavior, or predicting future events based on past observations (Jiménez et al., 2018).

Hydrological models are simplified representations of the terrestrial hydrological cycle, serving as essential tools in various hydrological applications, from flood management and agricultural planning to dam design and climate change impact studies (K. J. Beven, 2012). Their core purpose is to enhance understanding of hydrological systems and generate testable predictions, often extending beyond observed data to encompass short-term and long-term scenarios and simulate additional variables. These models recognize the inherent complexity of catchments, where unique physical characteristics at each location determine specific hydrological responses (K. J. Beven, 2012). Predicting these responses, particularly streamflow, is crucial for various research and operational activities. Hydrological models are built upon assumptions of universality, allowing a single model to represent multiple similar systems, and physical realism, meaning model components correspond to real-world entities (Wagener & Gupta, 2005). However, representing real-world environmental systems presents challenges, including scaling measurements, defining boundary and initial conditions, and characterizing the physical, chemical, and biological properties of the modeling domain (K. Beven, 2009).

The evolution of hydrological modeling has progressed from simple models like the unit hydrograph (Dooge, 1959) and the rational formula (Dooge J., 1957) to more complex representations. The development of the Stanford Watershed model, leading to the Sacramento model (Burnash, 1995), enabled continuous time representation of rainfall-runoff. Spatially explicit, physically based models like the SHE model (Abbott et al., 1986) aimed to estimate parameters directly from observable characteristics. The ideal model balances accuracy and simplicity, using minimal parameters and complexity to achieve realistic results (Wheater et al., 2007). Hydrological models describe the physical processes transforming precipitation into streamflow, encompassing components like evapotranspiration, surface runoff, and groundwater flow (Setegn et al., 2008). Their complexity ranges from simple unit hydrograph-based models to those based on dynamic flow equations, simulating processes like canopy interception, evaporation, and subsurface flow (Setegn et al., 2008).

Hydrological models can be classified based on several criteria, including their structure, underlying principles, and intended applications. This classification system helps researchers and practitioners select the most appropriate model for a given hydrological study and understand its operational mechanisms.

One common classification distinguishes models based on their representation of physical processes. Physically based models simulate hydrological processes using fundamental physical laws and principles, offering a detailed representation of the hydrological cycle (Yimam, 2023). Conceptual models, while still parametric, employ simplified representations of hydrological processes, focusing on key components without the need for detailed physical descriptions (Yimam, 2023). Empirical models, also known as data-driven models, rely solely on observed data to establish relationships between hydrological variables, often neglecting the underlying physical processes (Yimam, 2023).

Another classification considers the spatial distribution of model parameters and calculations. Lumped models treat the catchment as a single, homogeneous unit, averaging inputs and outputs over the entire area (Maskey, 2022). Distributed models, conversely, account for spatial variability by simulating processes at various locations within the catchment, capturing the heterogeneity of the landscape (Maskey, 2022). Semi-distributed models represent a compromise between these two approaches, incorporating some degree of spatial variability while maintaining a level of simplification for computational efficiency (Maskey, 2022). While these classifications provide a structured framework for

understanding hydrological models, it's crucial to recognize that model selection often involves trade-offs between model complexity, data requirements, and the specific hydrological questions being addressed. The optimal choice depends on the specific goals of the study and the available resources.

2.4 Soil and Water Assessment Tool (SWAT) model

2.4.1 Overview of the model

The Soil and Water Assessment Tool (SWAT) model is a computer simulation used to predict the quality and quantity of surface and groundwater resources within a watershed. It focuses primarily on the environmental impacts of land use, land management practices, and climate change on water resources within large, complex areas like river basins (Neitsch et al., 2009). Developed by the USDA Agricultural Research Service and Texas A&M AgriLife Research, SWAT provides a comprehensive framework for analyzing the hydrological cycle and its interactions with land management (Neitsch et al., 2009).

SWAT simulates various hydrological processes, including runoff, infiltration, evapotranspiration, groundwater flow, and nutrient loading (Islam et al., 2021). This allows for assessments of the impacts of different land management scenarios on water quantity and quality. The model operates at a large watershed scale, enabling analysis of entire river basins and understanding the cumulative effects of land use changes and management practices across extensive areas (Neitsch et al., 2009). SWAT is commonly used to evaluate the effectiveness of conservation practices like soil erosion control, non-point source pollution mitigation, and sustainable agricultural practices, providing valuable information for informed decision-making in water resource management (Yuan & Koropeckyj-Cox, 2022).

The Soil and Water Assessment Tool (SWAT) enhances hydrological modeling and management by dividing watersheds into smaller, manageable units. In SWAT, a watershed is first divided into multiple sub-watersheds, which are then further subdivided into Hydrologic Response Units (HRUs). These HRUs represent unique combinations of land use, management practices, and soil characteristics within a sub-watershed (P. W. Gassman et al., 2007). While HRUs represent percentages of the sub-watershed area and are not spatially identified within a standard SWAT simulation, they serve as the fundamental building blocks of the model. Alternatively, a watershed can be subdivided only into sub-watersheds characterized by dominant land use, soil type, and management (P. W. Gassman

et al., 2007). By modeling each HRU separately, SWAT facilitates a detailed analysis of hydrological processes and responses to management practices (Lee et al., 2024). The incorporation of HRUs allows the model to account for spatial variability in hydrological responses, improving the accuracy of predictions related to base flow and runoff (Lee et al., 2024). SWAT requires extensive input data, including digital elevation models, soil maps, land use data, and weather information, which are essential for accurately delineating HRUs (Bagul & Mohite, 2023). Integrating this geospatial data provides a comprehensive understanding of watershed characteristics, facilitating effective management strategies (Khalid et al., 2015). Model calibration and validation are critical, using metrics such as R^2 and NSE to assess performance (Tenaw et al., 2024). The calibrated model can then simulate various management scenarios, helping to identify effective strategies for sediment yield reduction and erosion control (Tenaw et al., 2024).

The SWAT model requires a diverse range of input data to effectively simulate complex hydrological processes. Daily rainfall, maximum and minimum air temperatures, solar radiation, relative humidity, and wind speed are essential meteorological inputs, driving the model's simulation of water and sediment circulation, vegetation growth, and nutrient cycling. These data, particularly precipitation and mean daily temperature, also inform estimations of snowfall rates. Geographic data, including a Digital Elevation Model (DEM), land use/land cover maps, and soil data, define the physical characteristics of the watershed, while Hydrologic Response Units (HRUs) homogeneous areas with unique combinations of land use, soil, and slope—represent spatial variability within the watershed. Human influences on hydrological processes are incorporated through management data, such as planting and harvesting dates, fertilizer and pesticide application rates, irrigation practices, and tillage operations. SWAT offers three methods for estimating evapotranspiration (ET): Hargreaves (requiring only temperature), Priestley-Taylor (using temperature and solar radiation), and Penman-Monteith (considered the most accurate and utilizing a comprehensive set of weather data).

2.4.2 Hydrological component of SWAT

SWAT simulates watershed hydrology in two phases: a land phase and a routing phase. The land phase simulates water movement within the landscape, determining the amount of water, sediment, nutrients, and pesticides entering the stream network. This involves processes like infiltration, evapotranspiration, runoff, and lateral flow, calculated within HRUs defined by land use, soil, and slope. The routing phase simulates the movement of

water and pollutants through the stream network. Driven by weather and geographic data, SWAT uses physically-based and empirical equations to calculate these processes, ultimately providing insights into water quantity and quality under various management scenarios.

SWAT's watershed simulations rely on accurate water balance modeling. This is crucial for predicting the movement of substances like pesticides, sediments, and nutrients, as the simulated hydrologic cycle must reflect real-world conditions. The land phase of this cycle determines the amount of water, sediment, nutrients, and pesticides entering the main channel from each sub-basin. SWAT bases its hydrologic cycle simulation on the water balance equation.

$$\mathrm{SWt} = \mathrm{SWo} + \sum_{i=1}^{t}(Rday - Qsurt - Ea - Wsweep - Qgw) \qquad 2\text{-}1$$

The final soil water content (SWt) is calculated by considering the initial soil water content (SW0) and the changes due to precipitation (Rday), surface runoff (Qsurf), evapotranspiration (Ea), water entering the deeper soil layers (wseep), and return flow from groundwater (Qgw) over a given period (t).

When rainfall exceeds infiltration, surface runoff occurs. SWAT offers two estimation methods: the SCS curve number method (United States Soil Conservation, 1972) and the Green & Ampt method (Heber Green & Ampt, 1911). While the Green & Ampt method is more accurate, its need for sub-daily data made it unsuitable for this study, leading to the adoption of the simpler SCS curve number method. This method provides a consistent way to estimate runoff based on land use and soil type (Rallison & Miller, 1982). The SCS curve number method calculates runoff in the following way:

$$Qsurf = \frac{(R_{day} - Ia)^2}{(R - I_{a-s})} \qquad 2\text{-}2$$

Qsurf, the accumulated runoff, is calculated based on Rday, the daily rainfall, after accounting for initial losses (Ia, which includes surface storage, interception, and initial infiltration) and a retention parameter (S).

The SCS curve number method considers three antecedent moisture conditions: dry (I), average (II), and wet (III). The curve number for dry conditions (I) represents the lowest possible daily value. Equations 2-3 and 2-4 are used to calculate the curve numbers for conditions I and III, respectively.

$$CNI = CNII - \frac{20\times(100-CNII)}{(100-CNII+exp[2.533-0.0636\times(100-CNII)])} \quad 2\text{-}3$$

$$CNIII = CNII \times exp\left(0.0636 \times (100 - CNII)\right) \quad 2\text{-}4$$

The terms CNI, CNII, and CNIII represent the curve numbers for moisture conditions I (dry), II (average), and III (wet), respectively. The retention parameter is calculated using Equation 2-5.

$$S = 25.4 \times \left(\frac{1000}{CN} - 10\right) \quad 2\text{-}5$$

The curve number (CN) used in hydrological calculations depends on the land use, soil permeability, and how wet the soil was before the rainfall event (antecedent soil water condition). A common simplification for initial abstraction (Ia) is 0.2 times the potential maximum retention (S). Using this approximation, the original equation can be rewritten in a simplified form in equation (2-6).

$$Qsurf = \frac{(Rday-0.25)^2}{R+0.85} \quad 2\text{-}6$$

Peak runoff rate, the maximum runoff flow during a rainfall event, indicates a storm's erosive power and helps predict sediment loss. Using a modified rational method, the SWAT model calculates this rate for each Hydrologic Response Unit (HRU) (Neitsch et al., 2009).

$$Q_{peak} = \frac{a_{tc}\times Q_{sur}\times A}{3.6\times t_{conc}} \quad 2\text{-}7$$

In the above equation, the peak runoff rate (Qpeak, measured in cubic meters per second) is calculated using several factors: the fraction of daily rainfall occurring during the time of concentration (atc), the surface runoff (Qsurf, in millimeters), the sub-basin area (A, in square kilometers), and the time of concentration (tconc, in hours). The constant 3.6 is a unit conversion factor to reconcile the different units and express Qpeak in m^3/s.

SWAT calculates the fraction of daily rain falling during the period of highest rainfall intensity (atc) using the following formula:

$$atc = 1 - exp(2 \times t_{conc} \times ln(1 - a_{0.5})) \quad 2\text{-}8$$

Where atc represents the fraction of daily rainfall occurring within the half-hour of highest intensity and tconc is the time of concentration for the sub-basin, measured in hours.

The time of concentration (tconc) represents the time it takes for water from the most distant point in a sub-basin to reach the outlet. It's calculated by adding the time it takes for overland flow to reach a channel (tov) and the time it takes for the water to travel through the channel network to the outlet (tch). Therefore, tconc is the sum of these two components: overland flow time and channel flow time.

$$t_{conc} = t_{ov} + t_{ch} \quad 2\text{-}9$$

The provided equations detail how SWAT calculates the components of the time of concentration:

$$t_{ov} = \frac{L_{slp}}{3600 \times V_{ov}} \quad 2\text{-}10$$

$$t_{ch} = \frac{L_c}{3.6 \times V_c} \quad 2\text{-}11$$

The provided information clarifies the variables used in the time of concentration calculations:

- Lslp: Average slope length of the sub-basin, measured in meters. This is the distance water travels overland.
- Vov: Overland flow velocity, measured in meters per second.
- Lc: Average channel length, measured in kilometers. This is the distance water travels within the channel network.
- Vc: Average channel flow velocity, measured in meters per second.
- 3600: Conversion factor from seconds to hours, used in the tov calculation.
- 3.6: Conversion factor from meters per second to kilometers per hour, used in the tch calculation.

These variables, along with the equations provided previously, allow for the calculation of tov (overland flow time) and tch (channel flow time), which are then summed to determine the total time of concentration (tconc).

The second phase of the hydrological cycle, routing, involves the movement of water through the watershed's channel network. This process transports not only water but also sediment, nutrients, and pesticides towards the outlet. The model accounts for changes in channel dimensions over time due to erosion (downcutting) and widening. Similar to overland flow calculations, Manning's equation is used to determine the flow rate and velocity in the channels. The channel cross-section and slope are derived from the Digital Elevation Model

(DEM) data. The model simplifies the main channels (reaches) by assuming a trapezoidal shape.

SWAT offers two methods for routing flow through channel networks: the variable storage method and the Muskingum method. Both are derived from the kinematic wave model. The variable storage method employs a straightforward continuity equation to track changes in storage volume. The Muskingum method, on the other hand, represents channel storage as a combination of prism storage (water stored above the normal channel depth) and wedge storage (water stored due to changes in flow depth along the channel). During channel flow calculations, the model accounts for transmission losses and evaporation. This approach, based on the continuity equation, is supported by Williams & Hann, (1973) and J. G. Arnold et al.,(2012). The storage routing method's foundation is the continuity equation.

$$\Delta V_{stored} = V_{in} - V_{out} \qquad 2\text{-}12$$

Equation 2.12, describes the change in storage volume within a channel reach during a given time step. It states that the change in stored volume (ΔVstored, in cubic meters) equals the difference between the inflow volume (Vin, in cubic meters) and the outflow volume (Vout, in cubic meters) during that time step. The above equation can be rewritten as follows:

$$\Delta V_{stored2} - \Delta V_{stored1} = \Delta t \times \left(\frac{q_{in.1}+q_{in.2}}{2}\right) - \Delta t \times \left(\frac{q_{out.1}+q_{out.2}}{2}\right) \qquad 2\text{-}13$$

Where:

- Vstored1: Storage volume at the beginning of the time step (m^3).
- Vstored2: Storage volume at the end of the time step (m^3).
- Δt: Length of the time step (seconds).
- qin1: Inflow rate at the beginning of the time step (m^3/s).
- qin2: Inflow rate at the end of the time step (m^3/s).
- qout1: Outflow rate at the beginning of the time step (m^3/s).
- qout2: Outflow rate at the end of the time step (m^3/s).

Equation 2-14 provides a more comprehensive water balance calculation for a channel reach, incorporating additional factors beyond simple inflow and outflow:

$$V_{stored2} = V_{stored1} + V_{in} - V_{out} - t_{loss} - E_{ch} + div + V_{bnk} \qquad 2\text{-}14$$

Where:

- Vstored2: Volume of water in the reach at the end of the time step (m^3).
- Vstored1: Volume of water in the reach at the beginning of the time step (m^3).
- Vin: Volume of water flowing into the reach during the time step (m^3).
- Vout: Volume of water flowing out of the reach during the time step (m^3).
- tloss: Volume of water lost from the reach through transmission through the bed (m^3).
- Ech: Volume of water lost due to evaporation from the reach during the day (m^3).
- div: Volume of water added to or removed from the reach during the day (m^3) - this represents external diversions or additions.
- Vbnk: Volume of water added to the reach from bank storage return flow (m^3).

This equation accounts for gains and losses of water within the reach due to various processes, making it a more realistic representation of channel water balance. It considers transmission losses, evaporation, external diversions, and return flow from bank storage, in addition to the inflow and outflow.

2.4.3 Sediment Component of SWAT

The SWAT model quantifies sediment yield at the HRU level using the Modified Universal Soil Loss Equation (MUSLE). Developed by R. Williams & D. Berndt, (1977) , MUSLE represented a significant advancement over the original USLE by replacing the rainfall erosivity factor with a runoff factor. This innovation allows for a more accurate estimation of soil erosion on a storm-by-storm basis, as sediment transport is a direct function of runoff, not rainfall alone (Neitsch et al., 2009).

The runoff factor in MUSLE is derived from the total runoff volume and peak discharge rate, which directly influence sediment transport and allow the model to capture spatial variations in erosion more effectively under dynamic watershed conditions. This addresses a key limitation of the USLE, which was primarily designed for long-term averages and does not directly account for runoff. The general form of the MUSLE equation used within SWAT is:

$$Sed = 1.18 \times (Q_{sur} \times Q_{Peak} \times A_{HRU})^{0.56} \times K_{USLE} \times C_{USLE} \times P_{USLE} \times LS_{USLE} \times CFRG \quad 2\text{-}15$$

The provided equation details the components of the Modified Universal Soil Loss Equation (MUSLE) used in SWAT:

Where:

- Sed: Sediment yield on a given day (metric tons).
- The term ($Q_{surf} \cdot Q_{peak} \cdot area_{hru}$) represents the runoff factor, where Q_{surf} is the surface runoff volume (mm), Q_{peak} is the peak runoff rate (m^3/s), and $area_{hru}$ is the HRU area (ha).
- K_{USLE} is the soil erodibility factor, which quantifies the inherent susceptibility of the soil to erosion.
- C_{USLE} is the cover and management factor, reflecting the influence of vegetation and agricultural practices.
- P_{USLE} is the support practice factor, accounting for erosion control measures like contouring or terracing.
- LS_{USLE} is the topographic factor, which combines the effects of slope length and steepness on erosion potential.
- CFRG is the coarse fragment factor, adjusting for the presence of rock fragments in the soil.

This equation allows SWAT to predict daily sediment yield by integrating the erosive power of a storm event with the physical characteristics of the landscape. While MUSLE offers significant improvements for event-based predictions, it is an empirical model, and some researchers note that it still lacks a comprehensive physical explanation of sediment transport processes(Tsige & Malcherek, 2024).

2.4.4 Advantages and Disadvantages of the SWAT

The Soil and Water Assessment Tool (SWAT) presents both significant advantages and disadvantages for hydrological modeling and ecosystem service evaluation. Its strengths lie in its comprehensive simulation capabilities, adaptability, and continuous development. SWAT effectively models complex hydrological processes, including runoff and non-point source pollution, making it suitable for diverse applications (Janjić & Tadić, 2023). Furthermore, it aids in quantifying the economic value of ecosystem services, supporting informed environmental management decisions (Garcia, 2023). The model's adaptability to various environmental conditions is enhanced by its ability to simulate human activities and agricultural practices (Janjić & Tadić, 2023). However, SWAT also has notable weaknesses. A primary limitation is its extensive data requirements, which can restrict its applicability in data-scarce regions (Akoko et al., 2021a; Janjić & Tadić, 2023). The complexity of model parameterization and calibration can also pose challenges for users, introducing uncertainties in predictions (Akoko et al., 2021a). Additionally, limitations in modeling reservoir

operations can affect the development of effective water management strategies (Jordan et al., 2022). Therefore, while SWAT offers a powerful tool for hydrological modeling, effectively balancing its data requirements and complexity is crucial for optimizing its application in environmental management.

The heavy data requirement of the SWAT model presents a significant challenge in the specific context of Somaliland. The region is characterized by a sparse network of meteorological stations, often with missing values, which complicates the creation of reliable, long-term weather inputs for hydrological modeling (Omer, 2024). This lack of a dense observational network is a well-documented issue that necessitates the use of satellite-based precipitation products like CHIRPS to fill data gaps. Furthermore, a complete absence of Public River gauging stations means there is no continuous streamflow and sediment data available for model calibration and validation.

This profound data scarcity renders it impossible to develop a locally calibrated SWAT model using standard procedures, a challenge also noted in other data-limited, semi-arid regions where the lack of adequate observational data hinders the establishment of a hydrological model. This critical limitation, therefore, directly necessitates the adoption of a regionalization methodology (Koycegiz & Buyukyildiz, 2019). In this approach, hydrological and sediment parameters are transferred from a data-rich, analogous catchment to the ungauged Humbo Weyne basin. Regionalization is not merely an alternative approach in this context; it is the essential scientific solution required to apply a powerful modeling tool to address the urgent issue of reservoir sedimentation.

2.4.5 Spatial proximity method of regionalization

Regionalization in hydrological modeling is crucial for estimating parameters in ungauged basins by leveraging data from gauged basins, improving the accuracy of hydrological simulations, especially in data-scarce regions (Kuana et al., 2023). This is essential for hydrological models like SWAT, particularly when dealing with ungauged or poorly gauged watersheds. One approach to regionalization is the spatial proximity method, which assumes that hydrologically similar basins are likely to be geographically close. This method is based on the principle that nearby catchments often share similar climatic, geological, and land use characteristics, influencing their hydrological response.

In the context of SWAT model parameterization, the spatial proximity method involves identifying a gauged basin or multiple basins that is geographically closest to the ungauged

target basin. The calibrated parameter values from the gauged basin(s) are then transferred to the ungauged basin. This can be a simple direct transfer or involve weighting the parameter values based on the distance or other similarity metrics between the basins (Steinschneider et al., 2015). While this method is relatively simple to implement, it relies on the assumption of strong spatial correlation in hydrological behavior. It is most effective when the gauged and ungauged basins are indeed hydrologically similar and located within a relatively homogeneous region. Limitations include potential overfitting to local variations in the gauged basin and the possibility that important hydrological differences between basins are not captured by simple proximity. Despite these limitations, the spatial proximity method was selected for this study of the Humbo Weyne catchment due to its straightforward application and the profound scarcity of the detailed physiographic data required for more complex regionalization techniques.

CHAPTER THREE: MATERIALS AND METHODS

The present study concerns the modeling of sediment yield for the Humbo Weyne Dam watershed to assess reservoir sedimentation risks. Therefore, in this chapter, details of the development of the SWAT model, including the spatial and hydro-meteorological data required to set up the model, are discussed. Additionally, the regionalization approach used to address the ungauged nature of the catchment, along with the procedures involved in sensitivity analysis, calibration, and validation using the Gauged catchment, are presented in detail to ensure an accurate representation of the watershed's hydrological and sediment transport processes.

3.1 Description of the Study Area

3.1.1 The Ungauged Catchment: Humbo Weyne, Somaliland

The Humbo Weyne Dam is situated northeast of Hargeisa, Somaliland, and is fed by a catchment with an approximate drainage area of 1,270 square kilometers. The watershed, which encompasses the Marodi-jeh dry river and the city of Hargeisa, has an estimated population of 1,726,000 as of 2020 (Liu et al., 2024). Seasonal rivers and streams channel rainwater runoff from the surrounding areas into the dam's reservoir.

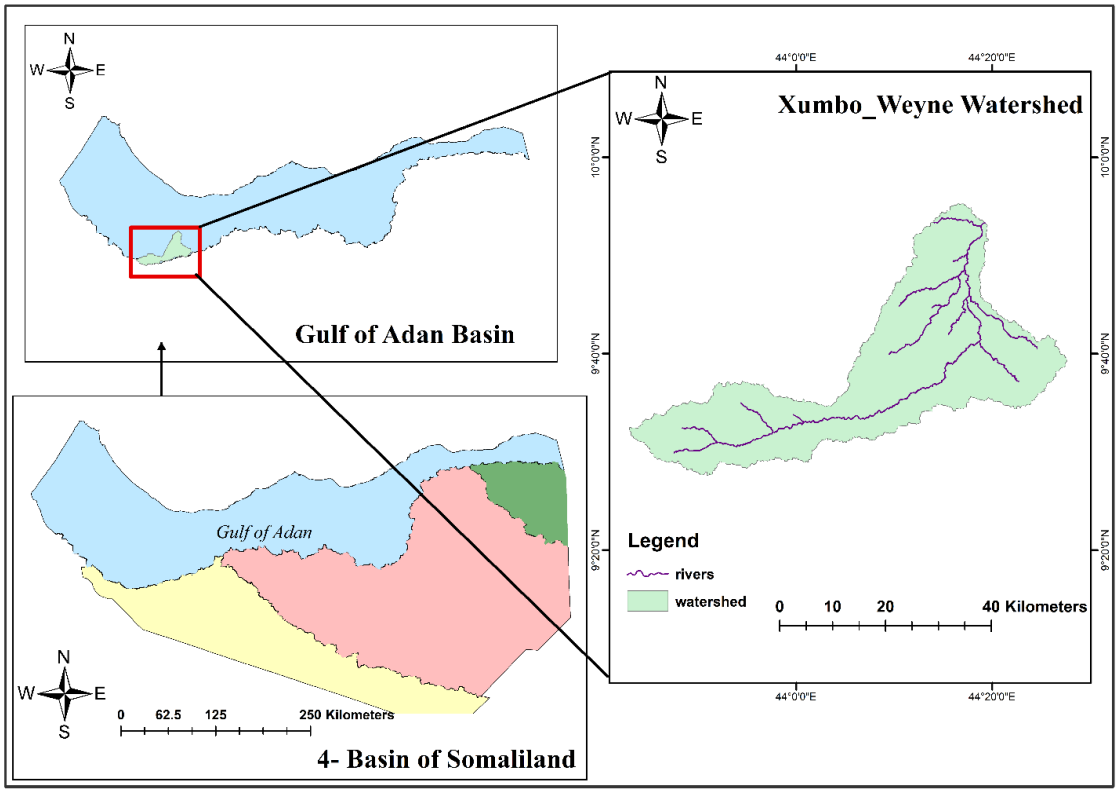

Figure 3-1: Humbo Wayne Dam watershed and its location in Somaliland river basins

3.1.1.1 Topography

The Humbo Weyne catchment is characterized by a varied topography with a significant elevation gradient, which is a key factor in its hydrological and erosional processes. The elevation within the watershed ranges from 877 m to 1693 m above sea level. As illustrated in Figure 3-2, the higher elevations are predominantly found in the southern and western parts of the catchment, gradually sloping down towards the lower plains in the northeast, where the dam is situated. The distribution of land across these elevation classes shows a clear pattern: the majority of the watershed lies at lower altitudes, with over 34% of the land below 1004 m and another 31% situated between 1004 m and 1145 m. Conversely, the higher, steeper regions are less extensive, with less than 3% of the catchment area located above 1464 m. This landscape, transitioning from steep upper regions to flatter lowlands, influences surface runoff patterns and helps identify potential areas of high erosive energy.

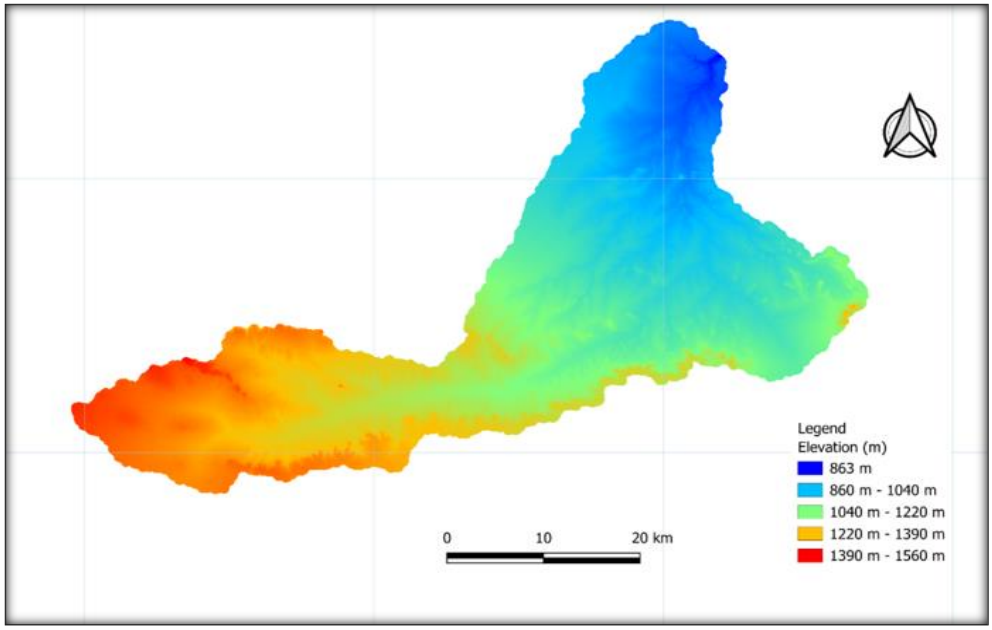

Figure 3.2: Topographic Map of the Humbo Weyne Catchment

3.1.1.2 Climate

The climate of the Humbo Weyne catchment is semi-arid, characterized by a distinct bimodal rainfall pattern and high temperatures throughout the year. Based on an analysis of six meteorological stations from 1995 to 2024, the mean annual precipitation for the catchment is 263.00 mm. The average daily maximum temperature is 30.92 °C, and the average daily minimum temperature is 17.21 °C.

As shown in Figure 3-3, the primary rainy season, known as the 'Gu', occurs from April to May, followed by a shorter rainy season, the 'Deyr', from August to September. There is significant inter-annual variability in rainfall, with a general increasing trend in total annual precipitation observed in the latter half of the record.

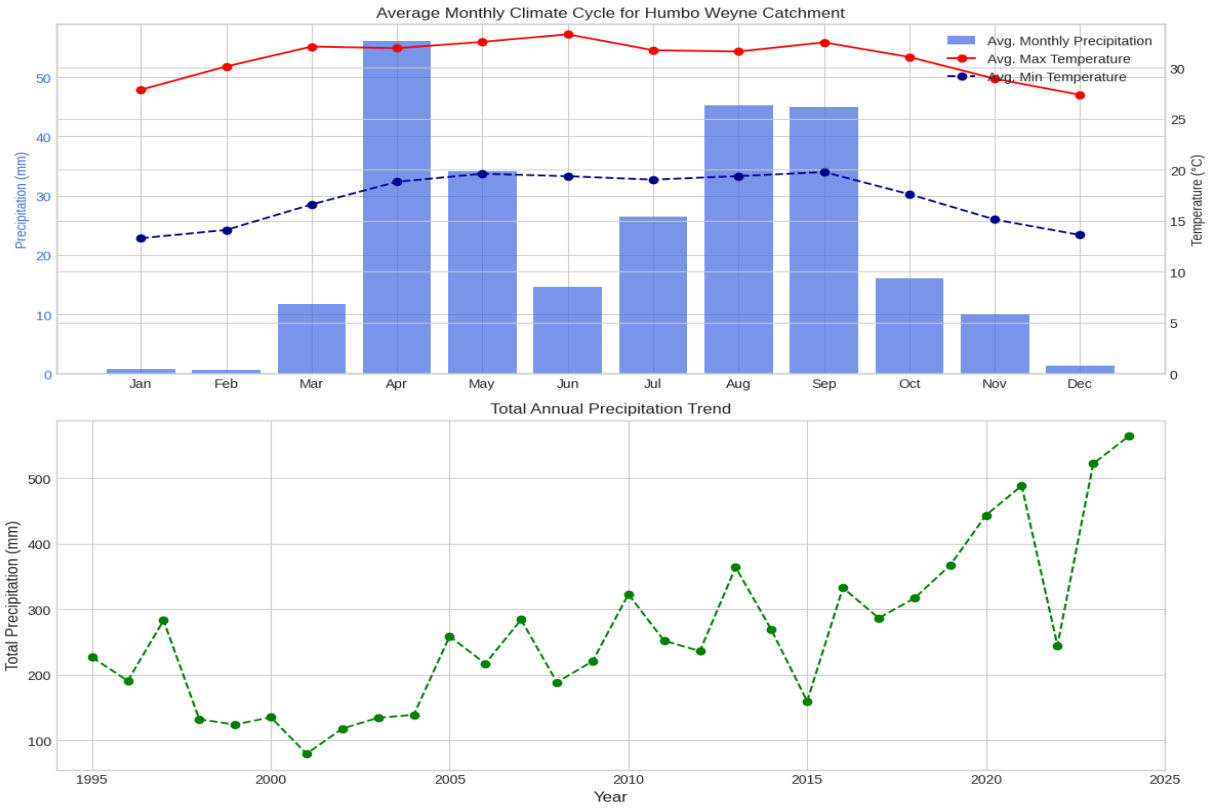

Figure 3-2 : Average Monthly Climate Cycle and Annual Precipitation Trend for the Humbo Weyne Catchment

3.1.1.3 Land Use/Cover

The land use and land cover (LULC) of the Humbo Weyne catchment are primary drivers of its hydrological and erosional response. The LULC distribution for this study was classified from satellite imagery, and the results indicate that the watershed is predominantly characterized by natural and semi-natural landscapes.

The Shrub land is the single largest LULC class, covering 51.9% of the total area. This is followed by Barren or Sparsely Vegetated land, which occupies 24.6%. Land used for grazing (Pasture) and cultivation (Agricultural Land) together account for just over 21% of the catchment. Urban areas and forests constitute the smallest portions of the landscape. The

spatial distribution of these classes, which was used as a key input for the SWAT model, is shown in Figure 3-4.

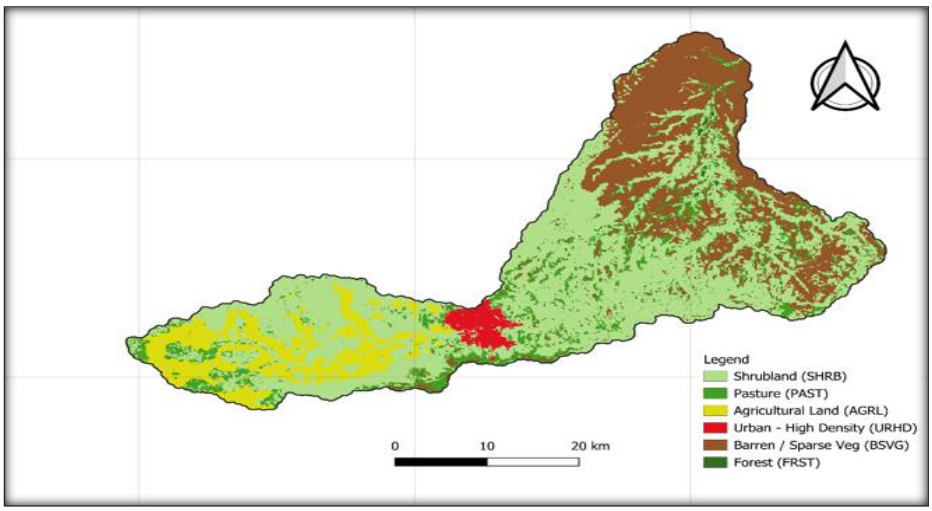

Figure 3-4: Land Use/Cover Map of the Humbo Weyne Catchment

3.1.1.4 Soil

The soil characteristics of the Humbo Weyne catchment were defined using the DSOLMap, with the spatial distribution of soil orders shown in Figure 3-4. The analysis reveals that the watershed is overwhelmingly dominated by Inceptisols, which cover 63.5% of the entire catchment area. These are young soils with minimal horizon development, common in a range of climates. Other significant soil orders present include Alfisols (16.4%) and Entisols (12.5%). The presence of these soil orders, which were a critical input for parameterizing the SWAT model, reflects the erosional and depositional environment of the region.

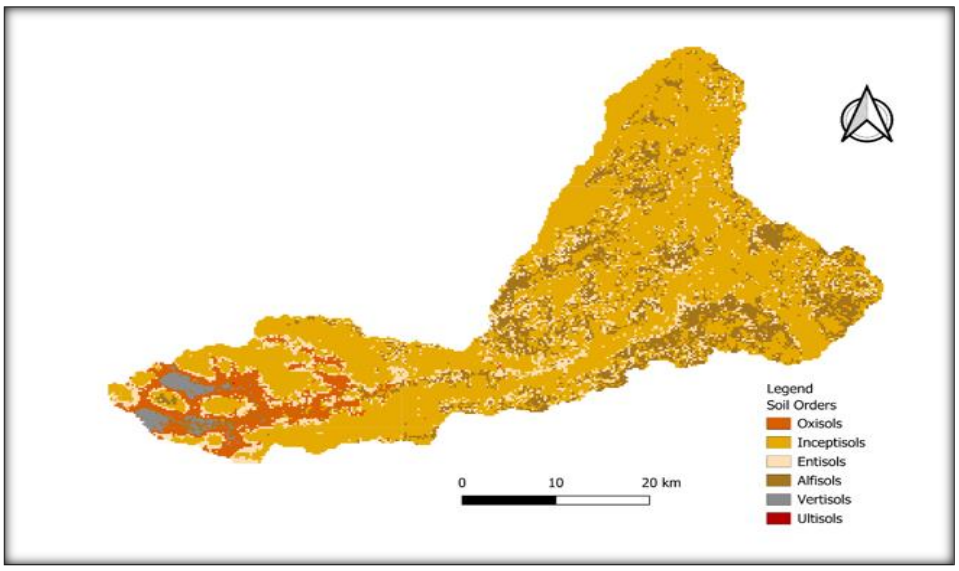

Figure 3-3: Soil Map of the Humbo Weyne Catchment

3.1.2 The Gauged Catchment: Gode catchment Wabi Shebelle, Ethiopia

The gauged catchment for this study is the upper Wabi Shebelle River basin, measured at the Gode gauging station in Ethiopia. This catchment was selected due to its geographic proximity and climatic similarity to the ungauged Humbo Weyne watershed, making it a suitable analogue for the regionalization of SWAT model parameters. The catchment covers a drainage area of 124,000 km². The topography is varied, with elevations ranging from 345 m at the outlet to 4,152 m in the headwaters. The climate is predominantly semi-arid, with a mean annual precipitation of 720 mm and average daily maximum and minimum temperatures of 28.4 °C and 15.8 °C, respectively. The most recent land cover assessment for 2020 shows that the area is primarily rangeland (55%) and agricultural land (31%). The dominant soil types are Cambisols and Luvisols.

3.2 Data Collection

3.2.1 Geospatial Data

Geospatial datasets are essential components for outlining the watersheds and identifying their physical characteristics in the SWAT model.

3.2.1.1 Digital Elevation Model (DEM)

Topography is characterized by a digital elevation model (DEM), which indicates the elevation of any point within a specified area at a certain spatial resolution. For this study, DEMs were obtained from the United States Geological Survey (USGS). A high-resolution 30-meter Shuttle Radar Topography Mission (SRTM) DEM was used for the ungauged Humbo Weyne catchment, while a 90-meter SRTM DEM was employed for the larger Gode gauged catchment. This data served as the primary input for watershed delineation and stream network generation, as well as the calculation of key topographic parameters such as sub-basin slope.

3.2.1.2 Soil Data

For the Gode catchment, soil spatial data was obtained from the FAO Digital Soil Map of the World (DSMW). To derive the necessary physical properties such as texture, bulk density, and hydraulic conductivity, the map was linked to the MWSWAT (MapWindow SWAT) soil database. This database contains a pre-formatted user soil lookup table that automatically populates the required multi-layer physicochemical parameters based on the standard FAO soil codes (e.g., Vertisols, Leptosols).

Humbo Wayne catchment, soil data was derived from the DSOLMap dataset. DSOLMap is a high-resolution global raster soil property map explicitly developed for the SWAT+ model. Unlike traditional vector-based maps which delineate soil types into polygons, DSOLMap provides continuous gridded data where each pixel contains specific soil property values derived from approximately 70,000 soil profiles in the WoSIS database.

This raster format allowed for a seamless integration with the 30m DEM used in the study, ensuring that every grid cell in the Humbo Wayne watershed was explicitly linked to a complete set of physical attributes (e.g., saturated hydraulic conductivity, available water capacity) required for precise hydrological modeling.

The resulting soil maps serve as the second major component for defining Hydrologic Response Units (HRUs). The physical properties extracted from these databases directly control the simulation of the water balance, including infiltration rates, subsurface storage, and percolation to shallow aquifers. Furthermore, parameters such as soil texture and organic carbon content were used to internally calculate the soil erodibility factor (K_{USLE}), which is the primary variable governing sediment yield calculations in the Modified Universal Soil Loss Equation (MUSLE).

3.2.1.3 Land Use/Land Cover (LULC) Data

The Land Use/Land Cover (LULC) data for both catchments were generated using the Copernicus Global Land Cover 100m map for the year 2020. This global dataset offers a detailed snapshot of the landscape's surface features. The raw data were downloaded and clipped to the respective watershed boundaries, and the original classes were then reclassified into specific categories required by the SWAT model, such as Shrub land (SHRB), Agriculture (AGRL), and Barren (BARR).

This processed LULC map is essential for the model setup, as it defines the surface components of the Hydrologic Response Units (HRUs). Each LULC class is assigned unique parameters within the SWAT model, such as runoff curve numbers and surface roughness coefficients. These parameters directly influence the model's simulation of surface runoff, evapotranspiration, and infiltration, making the LULC layer a critical driver of the water balance.

3.2.2 Climate Data

3.2.2.1 Gauged watershed (Gode Sub basin)

Daily meteorological data, including precipitation, minimum and maximum temperatures, wind speed, relative humidity, and solar radiation, were obtained from the Ethiopian Meteorological Institute (EMI). This study utilized data from three key meteorological stations: Ginir, Gode, and Harar (Table 3-1). In addition, monthly streamflow data for the Webi Shebelle River were acquired from the Ministry of Water, Irrigation, and Electricity at the Gode outlet for the period from 1990 to 2000. This discharge dataset serves as the foundation for calibrating and validating the SWAT model for the donor watershed.

Table 3-1: List and location of the Hydro-Meteorological stations within and around the Gode watershed.

No	station name	latitude	longitude	ELEVATION	Record Length in Years
1	Ginir	7.133333	40.706944	1941	1990-2020
2	Gode	5.932	43.5715	279	1990-2021
3	Harar	9.314433	42.093167	1977	1990-2022

A continuity check revealed significant data gaps across the station records from 1990 to 2022. Notably, the Ginir station was missing approximately 68.7% of its solar radiation and 58.9% of its relative humidity records, while the Gode station lacked nearly 37% of its wind speed data. To address these discontinuities and ensure a complete daily time series for the SWAT simulation, a hybrid bias-correction and gap-filling approach was employed:

Missing daily rainfall values were filled using bias-corrected CHIRPS satellite data. The CHIRPS data was corrected using the Random Forest Regression (RFR) method based on available observed days to ensure it matched the local station magnitude before being used to fill gaps. Gaps in maximum/minimum temperature, wind speed, and relative humidity were filled using ERA5 Reanalysis data.

This rigorous pre-processing ensured that the SWAT model was driven by a continuous, quality-controlled dataset that combined the accuracy of ground observations with the temporal completeness of global reanalysis products.

3.2.2.2 Ungauged watershed (Humbo Wayne)

A comprehensive daily meteorological dataset covering the period from 1995 to 2024 was created to support the SWAT model. To develop a reliable precipitation dataset, a hybrid approach was employed. Data from six local ground-based weather stations was complemented by the Climate Hazards Group InfraRed Precipitation with Station data (CHIRPS) satellite product to form a continuous time series. To ensure consistency and eliminate systematic bias between the satellite estimates and the ground observations, the quantile mapping technique was applied. This technique corrected the CHIRPS data based on the local station records, resulting in a final, continuous, and bias-corrected precipitation dataset.

Due to the absence of comprehensive local records for other parameters, daily data for maximum and minimum temperature, solar radiation, wind speed, and relative humidity were obtained from the ERA5 global reanalysis dataset. This combined methodology produced a complete and consistent set of daily weather inputs necessary for driving the SWAT simulation in the Humbo Weyne catchment.

3.2.2.3 Solar radiation

In instances where direct measurements of solar radiation data were unavailable, especially for historical station records, daily solar radiation values (Rs) were estimated using the Angstrom-Prescott formula. This widely used method, adopted from the Food and Agriculture Organization (FAO) (Allen & FAO, 1998), calculates solar radiation based on sunshine duration, which was accessible from the meteorological records.

The process began by calculating the daily extraterrestrial radiation (Ra) and the maximum possible sunshine duration (N) for the specific latitude and day of the year. The Angstrom-Prescott equation was then applied:

$$R_s = \left(a_s + b_s \frac{n}{N}\right) R_a \qquad \text{----------} \qquad 3\text{-}1$$

Where:

- Rs Is the calculated solar radiation ($MJ/m^2/day$).
- Ra Is the extraterrestrial radiation ($MJ/m^2/day$).
- n/N is the relative sunshine duration (dimensionless).
- a_s And b_s are the empirical Angstrom coefficients.

Since local calibration of these coefficients was not feasible, the standard values recommended by the FAO for an inland, arid, or semi-arid climate were used: $a_s = 0.25$ and $b_s = 0.50$ (Allen & FAO, 1998). This approach provided a complete and scientifically sound daily time series of solar radiation, which is an essential input for the SWAT model.

3.3 Data Quality Assessment

Before using the climate data as model input, a quality assessment was conducted to ensure the integrity and consistency of the time-series records. This critical step helps identify and address any non-climatic influences, such as changes in station location or instrument upgrades that could potentially bias the model results.

3.3.1 Homogeneity Testing

The homogeneity of the daily precipitation records from the meteorological stations was evaluated using the Rainbow software package (Raes et al., 2006). The primary method employed was the double-mass curve analysis (J. K. Searcy & C. H. Hardison, 1960), a graphical technique used to check the consistency of a station's data over time relative to its neighbors.

In addition to the visual inspection of the curve, the Rainbow software plots the cumulative deviation from the mean against statistical confidence limits (90%, 95%, and 99%). A deviation line crossing these limits would indicate a statistically significant inconsistency. For this study, the double-mass curve analyses for all six stations produced straight trend lines, and the cumulative deviation remained well within the 95% confidence limit. This provided both visual and statistical confirmation that the precipitation datasets were homogeneous and suitable for use in the SWAT model.

3.4 Spatial Data Processing

3.4.1 DEM Projection

The raw 30m SRTM Digital Elevation Model (DEM) was projected from the geographic coordinate system (GCS_WGS_1984) to the local projected coordinate system (UTM Zone 37N). This transformation is critical for preserving accurate area and distance properties required for watershed delineation.

3.4.2 Land Use and Soil Reclassification

SWAT cannot directly interpret global land cover codes. Therefore, the Copernicus Land Use map was reclassified into SWAT-specific 4-letter codes (e.g., mapping 'Shrubland' to 'RNGE'). Similarly, the FAO soil map was linked to a user-soil database (usersoil), assigning

physical properties such as texture, bulk density, and hydraulic conductivity to each raster value.

3.5 SWAT Model Setup

To simulate the hydrological processes and sediment yield, this research utilized two distinct SWAT modeling frameworks tailored to the specific data availability of the catchments. For the gauged catchment (Gode), the ArcSWAT 2012 model was employed to establish regional parameters. For the ungauged study area (Humbo Weyne), the SWAT+ model was selected to leverage its improved spatial representation and landscape routing capabilities.

3.5.1 Model Setup for the Gauged Catchment

The simulation for the gauged watershed was conducted using ArcSWAT 2012 within the ArcGIS 10.4 environment. The setup involved detailed data pre-processing steps to ensure the spatial inputs were compatible with the model's requirements.

3.5.1.1 Watershed Delineation

The projected DEM was loaded into the model interface. A flow direction and accumulation matrix was calculated using the D8 algorithm. The watershed outlet was manually defined at the gauging station location, and a threshold area of 5,000 ha was applied to discretize the watershed into sub-basins.

3.5.1.2 Hydrologic Response Unit (HRU) Analysis

The reclassified Land Use, Soil, and Slope maps were overlaid to define HRUs. The slope was discretized into five classes (0-5%, 5-10%, 10-15%, 15-30%, >30%). To improve computational efficiency, a 10% threshold was applied to land use, soil, and slope classes to eliminate minor units.

3.5.2 Model Setup for the Ungauged Catchment (Using SWAT+)

For the ungauged catchment, the SWAT+ modeling framework was employed. This choice was made because of the models flexible and detailed spatial representation, which is crucial for finer-scale analysis. Unlike the traditional SWAT model, which aggregates HRU outputs at the sub-basin level, SWAT+ allows for the routing of individual HRUs through distinct landscape units and channels, providing a more realistic simulation of sediment transport from fields to the main channel network.

3.5.2.1 Watershed Delineation

The delineation for this ungauged catchment was conducted using a higher-resolution 30m x 30m DEM, which is more suitable for the smaller size of the catchment and the detailed analysis required. Following standard procedures, the stream network and sub-basins were generated based on a specified threshold area of 5000 ha.

3.5.2.2 Landscape and Hydrologic Response Unit (HRU) Definition

The SWAT+ workflow was followed to define the spatial units. This process involved overlaying land use, soil, and slope maps to create Landscape Units (LSUs) and HRUs. The slope was categorized into five classes: (0-5%, 5-10%, 10-15%, 15-30%, and >30%). A key advantage of this setup is that each HRU can be defined as a distinct spatial object, enabling more precise routing of water and sediment through the landscape before reaching the main sub-basin channel.

3.5.3 Weather Data Input and Model Execution

For both models, the required weather data, including daily precipitation, maximum and minimum temperatures, solar radiation, wind speed, and relative humidity, were formatted and loaded into the SWAT weather databases. Location tables were used to link the climate data to the appropriate sub-basins. Once all input data were loaded and the databases were generated, the models were executed to produce the initial simulation output, which then served as the basis for subsequent sensitivity analyses, calibration, and validation. The SWAT model setup flow diagram is shown in Figure 3.4

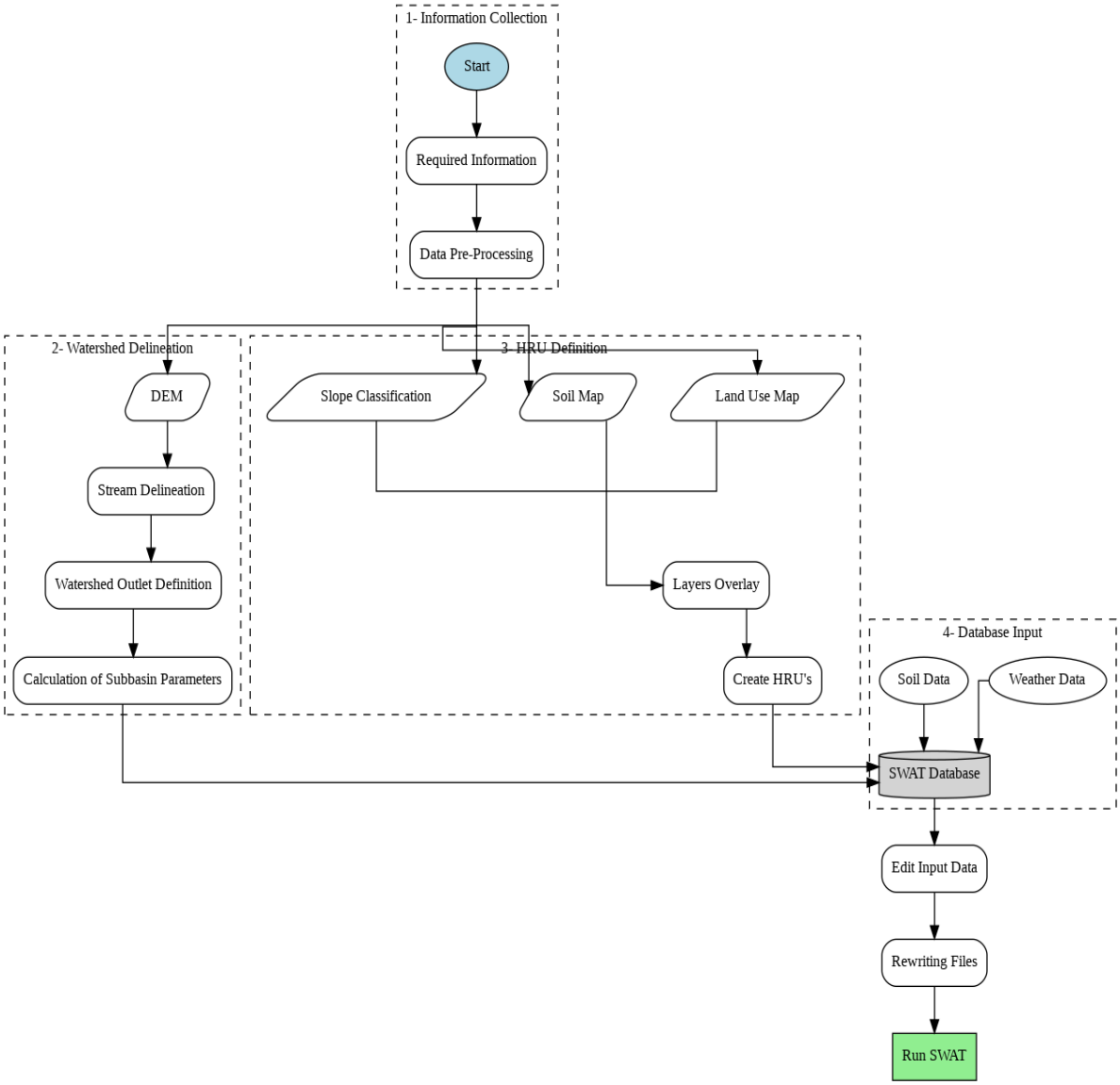

Figure 3-4: SWAT setup flow diagram

3.6 Model Calibration and Validation

To ensure that the model parameters accurately represent the regional hydrological processes, a rigorous calibration and validation procedure was performed on the gaged Gode catchment. This step is essential, as modern hydrological modeling practices emphasize the need for robust calibration to enhance model accuracy and reliability, particularly in data-scarce regions (Akoko et al., 2021b). The entire process utilized the SWAT-CUP software package (Abbaspour, 2015), which integrates the Sequential Uncertainty Fitting (SUFI-2) algorithm with the SWAT model.

The methodology employed in this study was systematically organized into three sequential stages: first, a sensitivity analysis was conducted to identify the key parameters influencing

the model; second, model calibration was performed to optimize these parameters; and finally, a model validation phase was implemented to assess the predictive capabilities of the model.

3.6.1 Sensitivity Analysis and Parameter Identification

The initial step in the calibration process was to identify the model parameters that significantly influence streamflow and sediment yield. Given the large number of parameters in SWAT, it is crucial to conduct a sensitivity analysis to focus calibration efforts on a manageable set of the most influential variables. This enhances efficiency and helps to manage model uncertainty (Moges et al., 2020).

The selection of initial parameters for the sensitivity analysis was guided by a comprehensive review of recent literature, particularly studies focusing on SWAT applications in Africa (Akoko et al., 2021). This approach ensured that the parameters chosen were relevant to the regional context. The final list of parameters considered for streamflow and sediment, along with their initial ranges, is presented in Tables 3-2 and 3-3.

A global sensitivity analysis was performed using SWAT-CUP and the SUFI-2 algorithm. SUFI-2 is recognized for its effectiveness in addressing uncertainties related to model structure, inputs, and parameters (Tang et al., 2021). The relative sensitivity of each parameter was assessed using a t-statistic and a p-value; a larger absolute t-stat and a p-value approaching zero indicate higher significance (Abbaspour, 2015).

Table 3-2: Parameters and Parameters ranges used in stream flow sensitivity analysis

Parameter Name	Recommended Range	Definition	Parameter Type
r_CN2.mgt	-0.20-0.20	SCS runoff curve number for moisture condition II	Surface runoff
v_ALPHA_BF.gw	0.0-1.0	Base flow alpha factor (days)	Groundwater
v_ALPHA_BNK.ret	0.0-1.0	Base flow alpha factor for bank storage	Groundwater
v_RCHARG_DP.gw	0.0-0.2	Deep aquifer percolation fraction	Groundwater
v_CANMX.hru	0.0-10.0	Maximum canopy index	Surface runoff
v_CH_K2.ret	0.0-150.0	Effective hydraulic conductivity in main channel alluvium (mm/hr)	Channel processes
v_CH_N2.ret	0.0-0.5	Manning's coefficient for channel	Channel process

r_SLSUBBSN.hru	-0.5-0.5	Average slope length	Geomorphology
v_TLAPS.sub	-10 - 10	Temperature laps rate (ºC/km)	Geomorphology
r_HRU_SLP.hru	0.0-0.2	Average slope steepness(m/m)	Surface runoff
v_REVAPMN.gw	0.0-500.0	Threshold depth of water in the shallow aquifer for revap to occur (mm)	Groundwater
v_SURLAG.bsn	0.0-10.0	Surface runoff lag time	Surface runoff
a_ESCO.hru	0.0-0.2	Soil evaporation compensation factor	Evapotranspiration
a_EPCO.hru	0.0-0.2	Plant evaporation compensation factor	Evapotranspiration
v_GW_DELAY.gw	0.0-50	Groundwater delay (days)	Groundwater
r_BIAI.crop.dat	2.0-8.0	Max leaf area index	Evapotranspiration
r_SOL_AWC.sol	-0.50-0.50	Available water capacity of the soil layer (mm/mm soil)	Soil water
r_SOL_K.sol	-0.50-0.50	Soil conductivity (mm/h)	Soil water
a_GW_REVAP.gw	-0.10-0.0	Groundwater revap coefficient	Groundwater
v_GWQMN.gw	0 - 2000	Threshold depth of water in the shallow aquifer required for return flow to occur (mm)	Groundwater
r_SOL_BD.sol	-0.50-0.50	Moist bulk density	Soil water
a_SOL_ALB.sol	0.75-1.50	Moist soil albedo	Soil water
r_Ov_N.hru	-0.2-0.0	Manning's value for overland flow	Surface runoff

Table 3-3: Parameters and Parameter range used in sediment yield sensitivity analysis

Parameter Name	Recommended Range	Definition	Parameter Type
a_PRF.bsn	0 – 0.2	Peak rate adjustment factor for sediment routing in the main channel	Channel
v_CH_D.rte	0 - 30	Average depth of main channel	Channel
v_CH_S2	-0.001 -10	Average slope of main channel	Channel
a_USEDL_P.mgt	0 - 0.20	USLE equation support practice	Sediment
v_SPCON.bsn	0 - 0.01	A linear parameter used in channel sediment routing	Channel
v_SPEXP.bsn	1.0 – 1.50	An exponent parameter used in channel sediment routing	Channel
a_USLE_K.sol	0 – 0.20	USLE equation soil erodibility (K) factor	Soil
r_HRU_SLP.hru	0 - 0.2	Average slope steepness	Surface runoff
a_CH_COV1.rte	0 - 0.2	Channel cover factor	Sediment
a_CH_COV2.rte	0 – 0.2	Channel erodibility factor	Sediment

r_CH_W2.rte	0 - 0.2	Average width of main channel	Channel
v_LAT_SED.hru	0 - 2	Sediment concentration in lateral flow and ground water flow	Sediment
a_USLE_C.Crop.data	0 – 0.2	Minimum value of USLE C-factor applicable to the land cover	Sediment
v_CH_WDR.rte	0 - 30	Channel width-depth ratio	Channel
a_ADJ_PKP.bsn	0 – 0.2	Peak rate adjustment factor for sediment routing in the subbasin	Channel
r_SLSUBBSN.hru	-0.5-0.5	Average slope length	Geomorphology

3.6.2 Model Calibration

Following the sensitivity analysis, the calibration focused on adjusting the most influential parameters to minimize the difference between simulated and observed historical data. The historical streamflow and sediment data for the Gode catchment were divided, with the period from 1995 to 1998 used for calibration. The SUFI-2 algorithm was executed for 500 simulations per iteration, systematically adjusting the parameter values within plausible ranges until the simulated monthly data closely matched the observed values from the Gode gauging station.

3.6.3 Model Validation

Model validation is the process of demonstrating that a calibrated model can make sufficiently accurate predictions using an independent dataset. The SWAT model for the Gode catchment was executed using the final optimized parameter set from the calibration phase. The simulated outputs were compared against the observed monthly streamflow and sediment data for the period from 1999 to 2000, which was not used during the calibration. The model's performance for both calibration and validation was quantitatively assessed to ensure its reliability before the parameters were transferred to the Humbo Weyne catchment.

3.7 Model Performance Evaluation

The performance of the SWAT model for the Gode donor catchment was quantitatively assessed during both the calibration and validation periods. This evaluation adhered to the recommended guidelines for systematically quantifying accuracy in watershed simulations, as outlined by D. N. Moriasi et al. (2007). A combination of graphical comparisons and statistical metrics was utilized to evaluate the model's accuracy. This study focused on four key metrics: the Nash-Sutcliffe Efficiency (NSE), Percent Bias (PBIAS), the RMSE-

observations standard deviation ratio (RSR), and the coefficient of determination (R^2). These metrics are widely used in SWAT applications (Bressiani et al., 2015).

Additionally, the SUFI-2 algorithm presents simulation results as an uncertainty band (the 95% Prediction Uncertainty band, or 95PPU). To assess the quality of this uncertainty analysis, we employed two specific metrics: the p-factor and r-factor. The overall performance of the model was evaluated based on ratings established by D. N. Moriasi et al.(2007), as presented in Table 3.4.

3.7.1 Nash-Sutcliffe Efficiency (NSE)

The Nash-Sutcliffe Efficiency (NSE) is a normalized statistic used to assess how well the plot of observed versus simulated data matches a 1:1 line. The NSE value ranges from negative infinity to 1.0, with 1.0 representing a perfect fit. A model simulation is generally considered satisfactory if the NSE is greater than 0.50 (D. N. Moriasi et al., 2007).

The NSE is calculated using the following formula:

$$NSE = 1 - \frac{\sum_{i=1}^{N}(O_i - P_i)^2}{\sum_{i=1}^{N}(O_i - \bar{O})^2} \quad \text{----------} \quad 3\text{-}2$$

Where:

- $\boldsymbol{O_i}$ Is the observed value
- $\boldsymbol{P_i}$ is the simulated value
- $\boldsymbol{\bar{O}}$ is the mean of observed data
- N Is the total number of observations.

3.7.2 Percent Bias (PBIAS)

Percent bias (PBIAS) measures the average tendency of the simulated data to be larger (overestimation) or smaller (underestimation) than the observed data. The optimal value is 0.0, with low-magnitude values indicating better model accuracy. Positive values indicate underestimation bias, while negative values indicate overestimation bias. A PBIAS within ±25% for streamflow and ±55% for sediment is typically considered satisfactory (D. N. Moriasi et al., 2007).

$$PBIAS = 1 - \frac{\sum_{i=1}^{N}(O_i - P_i)^2}{\sum_{i=1}^{N} O_i} \times 100 \quad \text{----------} \quad 3\text{-}3$$

3.7.3 Root mean square error observation standard deviation ratio (RSR)

RSR standardizes the Root Mean Square Error (RMSE) using the standard deviation of the observations. It varies from an optimal value of 0 (perfect simulation) to a large positive value. A lower RSR indicates a better model performance. Generally, a model simulation is considered satisfactory if RSR ≤ 0.70 (D. N. Moriasi et al., 2007).

$$RSR = \frac{\sqrt{\sum_{i=1}^{N}(O_i - P_i)^2}}{\sqrt{\sum_{i=1}^{N}(O_i - \bar{O})^2}} \quad 3\text{-}4$$

3.7.4 Coefficient of Determination (R^2)

The coefficient of determination (R^2) was used to describe the proportion of the variance in the observed data that is explained by the model. R^2 ranges from 0 to 1, with higher values indicating a better fit, and its use is widely documented in SWAT applications (Bressiani et al., 2015) .

It was recognized that R^2 alone can be misleading as it is insensitive to systematic over- or under-prediction (Krause et al., 2005). For this reason, modern model evaluation guidelines emphasize using R^2 in combination with other metrics like NSE and PBIAS to provide a more comprehensive assessment of model performance (D. N. Moriasi et al., 2007).

$$R^2 = \frac{\left[\sum_{i=1}^{N}(O_i - \bar{O})(O_i - P_i)\right]^2}{\sum_{i=1}^{N}(O_i - \bar{O})^2 \sum_{i=1}^{N}(P_i - \bar{P})^2} \quad 3\text{-}5$$

Where:

- $\boldsymbol{O_i}$ Is the observed value
- $\boldsymbol{P_i}$ is the simulated value
- $\boldsymbol{\bar{O}}$ is the mean of observed data
- $\bar{P}$ Is the mean of simulated data

3.7.5 Uncertainty Analysis Metrics (p-Factor and r-Factor)

To evaluate the quality of the calibration and its associated uncertainty, the p-factor and r-factor were used. The p-factor is the percentage of measured data points bracketed by the 95% Prediction Uncertainty band (95PPU). The r-factor measures the average thickness of the 95PPU band. A combination of a high p-factor and a low r-factor indicates a strong calibration.

Table 3-4: General Performance Ratings for Recommended Statistics (D. N. Moriasi et al., 2007)

Performance Rating	RSR	NSE	PBIAS (Streamflow)	PBIAS (Sediment)
Very Good	$0.00 \leq RSR \leq 0.50$	$0.75 < NSE \leq 1.00$	$PBIAS \leq \pm 10$	$PBIAS \leq \pm 15$
Good	$0.50 < RSR \leq 0.60$	$0.65 < NSE \leq 0.75$	$\pm 10 < PBIAS \leq \pm 15$	$\pm 15 < PBIAS \leq \pm 30$
Satisfactory	$0.60 < RSR \leq 0.70$	$0.50 < NSE \leq 0.65$	$\pm 15 < PBIAS \leq \pm 25$	$\pm 30 < PBIAS \leq \pm 55$
Unsatisfactory	$RSR > 0.70$	$NSE \leq 0.50$	$PBIAS > \pm 25$	$PBIAS > \pm 55$

3.8 Identification of Erosion Hotspots (Landscape Level)

To address the specific objective of determining the area most susceptible to erosion, this study leveraged the advanced spatial discretization capabilities of the SWAT+ model. Unlike traditional SWAT applications that aggregate sediment yield at the sub-basin level, this study analyzed sediment dynamics at the finer Landscape Unit (LSU) level. The calibrated SWAT+ model was used to simulate sediment transport for each of the 171 Landscape Units (LSUs) delineated within the Humbo Wayne watershed.

The average annual sediment yield (SYLD) for each LSU was extracted from the model output. This approach enables the precise identification of critical source areas, distinguishing between specific hillslopes, agricultural fields, or degraded shrublands that would otherwise be averaged out in a broader sub-basin analysis.

To prioritize areas for soil and water conservation interventions, the simulated sediment yield values for each LSU were categorized into erosion severity classes. This study adopted the classification scheme recommended by FAO-SWALIM (Omuto et al., 2009), which groups erosion rates into categories ranging from Low to Severe (Table 3-5). These classes were then mapped to visualize the spatial distribution of soil loss and explicitly identify the high-risk LSUs located on the northeastern escarpment.

Table 3-5: Sediment Yield Severity Classification

Sediment Yield (t/ha/yr)	Severity Class
0 – 5	Low
5 – 10	Moderate
10 – 20	High
20 – 30	Very High
> 30	Severe

CHAPTER FOUR: RESULTS AND DISCUSSION

The SWAT model was developed to quantify the magnitude of sediment yield and assess the spatial extent of soil erosion in the Humbo Wayne watershed, providing a scientific basis for sustainable reservoir management. Due to the lack of local monitoring data, model calibration and validation were performed using observed streamflow and sediment records from the spatially proximate gauged Gode catchment. In this section, the results are presented in detail, including the sensitivity analysis of key parameters, the model's performance evaluation on the gauged catchment, the simulated sediment influx to the Humbo Wayne reservoir, and the spatial identification of critical erosion hotspots to guide future conservation planning.

4.1 Rainfall-Runoff Relationship in the Watershed

The rainfall-runoff relationship within the Humbo Weyne watershed is illustrated in Figure 4.1. The hydrological response closely mirrors the region's bimodal climate regime. As shown in the flood hydrograph (Fig 4.1a), peak runoff events are consistently observed during the primary 'Gu' season (April–May) and the secondary 'Deyr' season (August–September).

Fig 4.1(a) depicts the shape of the hydrograph, which represents the watershed's integrated response to storm characteristics. Unlike catchments dominated by base flow where peak discharge may lag significantly behind peak rainfall, the Humbo Weyne watershed exhibits a rapid response. The steep rising limb of the hydrograph indicates a flashy system driven by high-intensity rainfall and limited infiltration capacity in the barren and shrubland areas. The recession limb, however, is controlled by the watershed's storage characteristics.

Overall, the water balance analysis reveals that out of the total annual average precipitation of 267.8 mm, approximately 88.64 mm drains out of the watershed as surface runoff. The remaining 66.3% is lost primarily to evapotranspiration and, to a lesser extent, deep percolation into the groundwater system. Due to the region's high temperatures and semi-arid climate.

To quantify the relationship between rainfall and runoff on a monthly basis, a regression analysis was performed using the simulated monthly data. As shown in Fig 4.1(b), a strong positive correlation was observed between monthly rainfall depth and runoff volume. The relationship is best described by a polynomial (quadratic) regression equation ($R^2 > 0.7$),

indicating that runoff generation is non-linear; as soil moisture storage fills up during the wet season, a higher percentage of rainfall is converted into runoff.

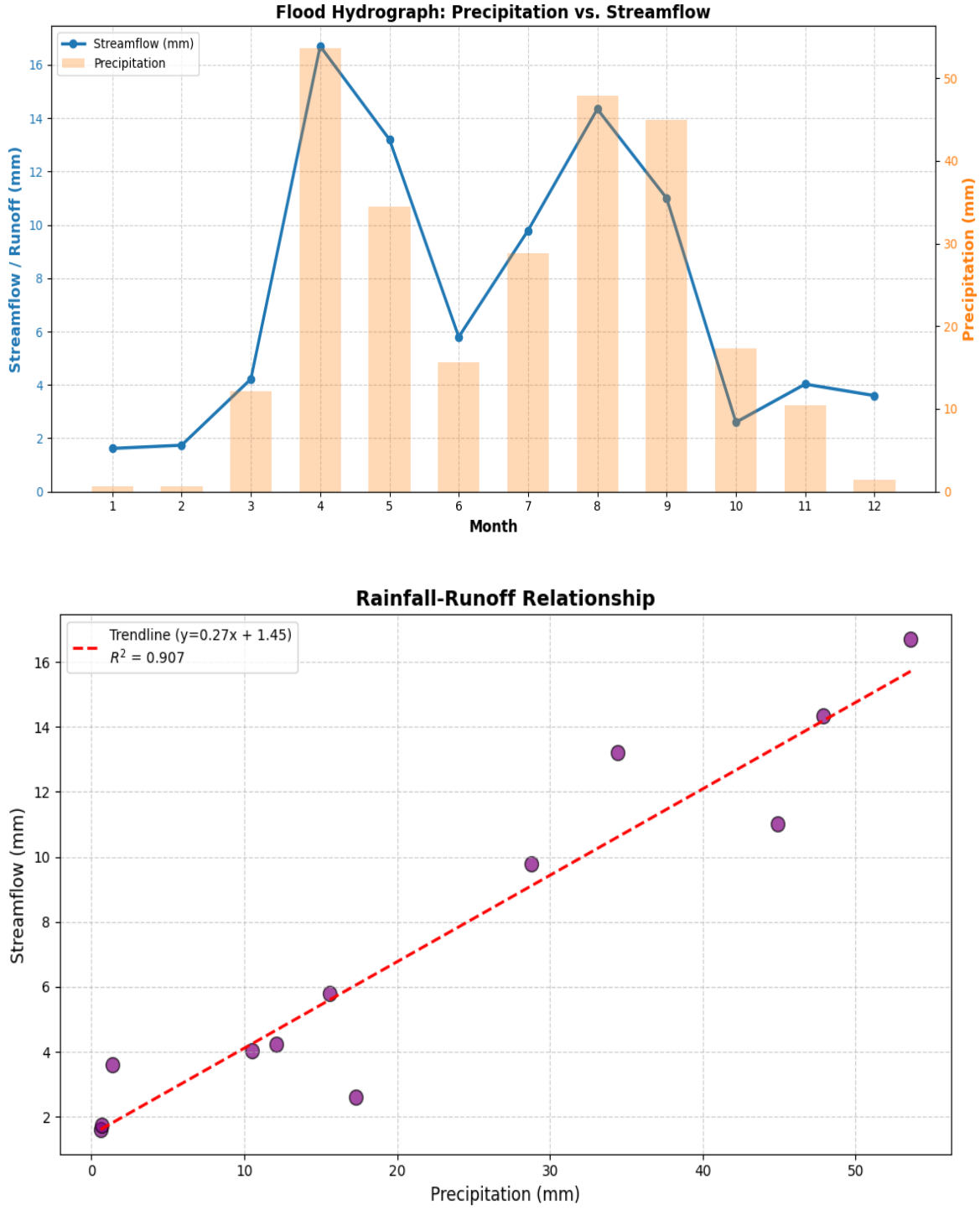

Figure 4-1: Rainfall-Runoff relationship of Humbo Weyne Watershed: (a) Flood hydrograph and (b) Monthly rainfall-runoff regression.

4.2 Watershed Delineation

The first critical step in the SWAT model development was the definition of the watershed boundaries, which naturally follow the topographic ridges. As indicated by (Cotter et al., 2003), the resolution of GIS data has a significant impact on model output uncertainty. Therefore, to minimize uncertainty associated with input data, the Humbo Weyne watershed, covering a total drainage area of 1,270 km², was delineated using a high-resolution 30m DEM.

Based on the topography and the stream network density, the watershed was subdivided into 17 sub-basins using a minimum threshold area of 5,000 ha. To further refine the spatial representation of erosion processes, these sub-basins were discretized into 171 Landscape Units (LSUs). This finer discretization allows the SWAT+ model to capture the heterogeneity of the landscape more effectively than traditional sub-basin aggregation (Aleksey Y Sheshukov et al., 2011)

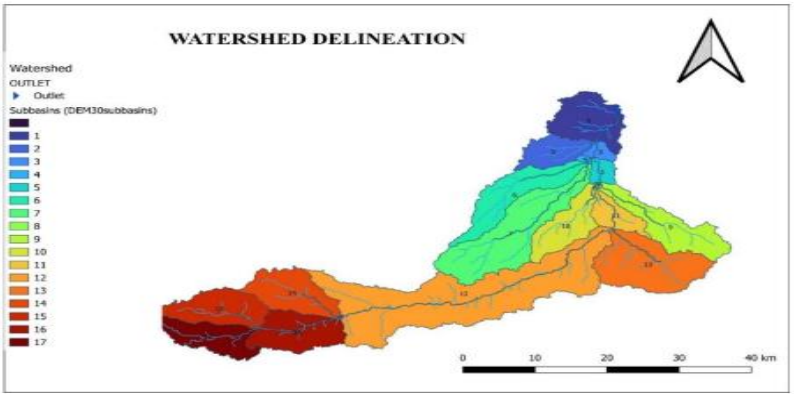

Figure 4-2: Delineated Humbo Weyne Watershed showing the 17 sub-basins and drainage network

4.3 Stream Flow Modelling

To estimate flows for the ungauged Humbo Weyne catchment, the model was first set up, calibrated, and validated on the spatially proximate gauged Gode catchment. The optimized parameters obtained from this process were subsequently transferred to the study area using the regionalization technique.

4.3.1 Sensitivity Analysis

A global sensitivity analysis was conducted using the Sequential Uncertainty Fitting (SUFI-2) algorithm within SWAT-CUP to identify the most influential parameters governing streamflow. The analysis evaluated the relative sensitivity of flow parameters based on their t-stat and p-value, where a larger absolute t-stat indicates higher sensitivity and a p-value closer to zero indicates greater significance. The results of the sensitivity analysis are presented in Figure 4.3.

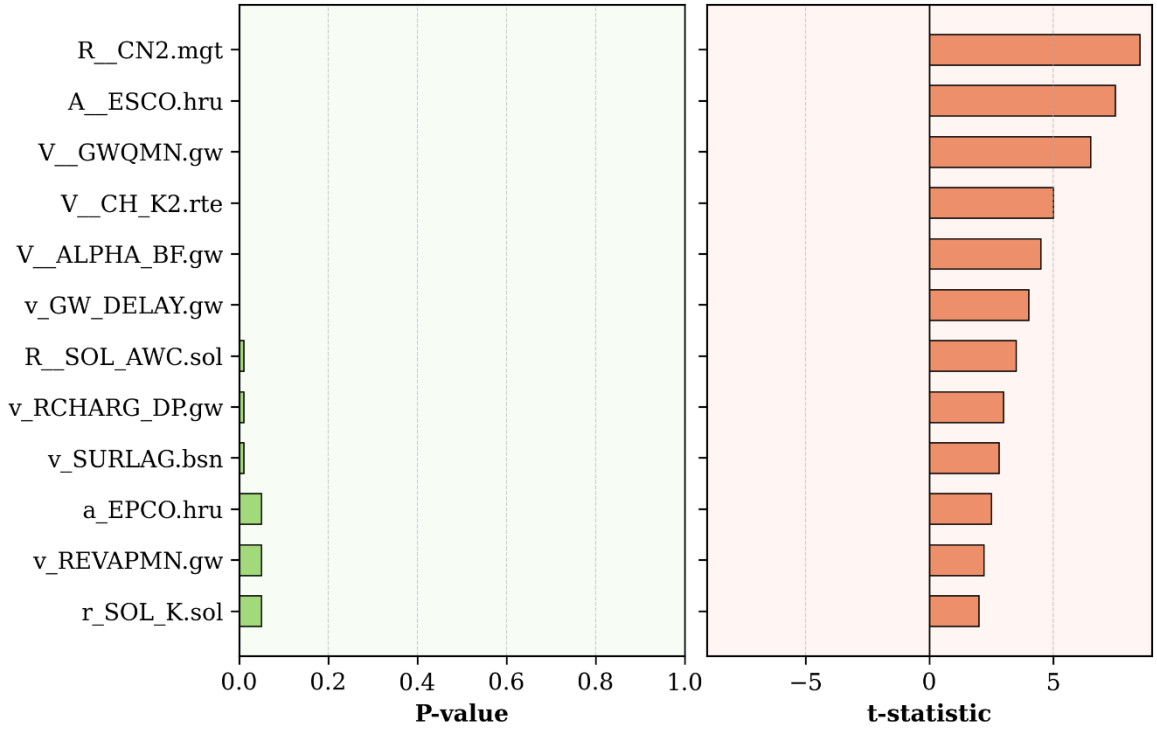

Figure 4-3: Global sensitivity analysis of streamflow parameters for the Gode catchment.

As shown in Figure 4.3, the SCS Runoff Curve Number (*R_CN2.mgt*) was identified as the most sensitive parameter (t-stat > 8, p-value = 0.00). This indicates that surface runoff generation in the region is highly dependent on land use, soil permeability, and antecedent moisture conditions. The Soil Evaporation Compensation Factor ($A\_ESCO.hru$) emerged as the second most sensitive parameter. This high ranking emphasizes the dominant role of evapotranspiration in the water balance, suggesting that the model is highly sensitive to how soil evaporation demands are met from different soil layers.

Groundwater parameters also demonstrated significant influence. The Threshold Depth for Return Flow ($V\_\_GWQMN.gw$) ranked third, highlighting the importance of the shallow aquifer's storage capacity in regulating base flow. This was followed by the Effective

Hydraulic Conductivity of the Main Channel ($V\_\_CH\_K2.rte$) as the fourth most sensitive parameter, which underscores the critical role of transmission losses in the river network—a characteristic typical of semi-arid ephemeral streams.

Other influential parameters included the Base flow Alpha Factor ($V\_\_ALPHA\_BF.gw$) and Groundwater Delay ($v\_GW\_DELAY.gw$), further confirming that the interaction between the aquifer and the stream is a key driver of the catchment's hydrology.

4.3.2 Model Calibration for Stream Flow

Model calibration was performed on a monthly time step for the period of 1995 to 1998. The SUFI-2 algorithm was used to optimize the sensitive parameters. The final fitted values, which resulted in the best simulation performance, are summarized in Table 4.2.

Table 4-1: Summary of calibrated flow parameters for the Gode catchment.

S/no	Parameter Name	Description	Fitted Value	Min Value	Max Value
1	R__CN2.mgt	SCS runoff curve number (Relative change)	-0.173	-0.2	0.2
2	A__ESCO.hru	Soil evaporation compensation factor	0.014	0	0.2
3	V__GWQMN.gw	Threshold depth of water in shallow aquifer (mm)	1464	0	2000
4	V__CH_K2.rte	Effective hydraulic conductivity of main channel (mm/hr)	52.19	0	150
5	V__ALPHA_BF.gw	Baseflow alpha factor (days)	0.45	0	1
6	V__GW_DELAY.gw	Groundwater delay time (days)	37.42	0	50
7	R__SOL_AWC.sol	Available water capacity of the soil layer	0.22	-0.5	0.5
8	v_RCHARG_DP.gw	Deep aquifer percolation fraction	0.08	0	0.2
9	v_SURLAG.bsn	Surface runoff lag time	7.56	0	10
10	a_EPCO.hru	Plant evaporation compensation factor	0.16	0	0.2
11	v_REVAPMN.gw	Threshold depth of water in the shallow aquifer for revap to occur (mm)	430	0	500
12	R__SOL_K.sol	Saturated hydraulic conductivity	0.19	-0.5	0.5

Note: 'R__' indicates a relative change where the current value is multiplied by (1 + value), 'V__' indicates a replacement with the specific value, and 'A__' indicates an absolute change.

The calibration results were evaluated visually and statistically. The statistical performance of the model during calibration is shown in Figure 4.5 and Figure 4.5.

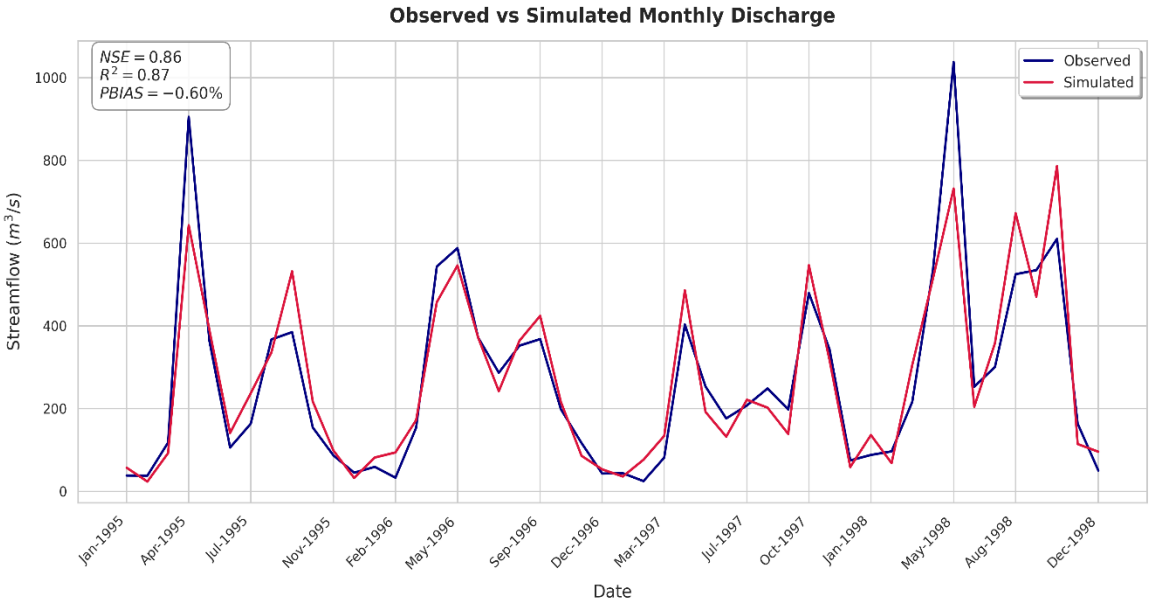

Figure 4-4: Observed vs. Simulated monthly streamflow hydrograph during calibration (1995–1998).

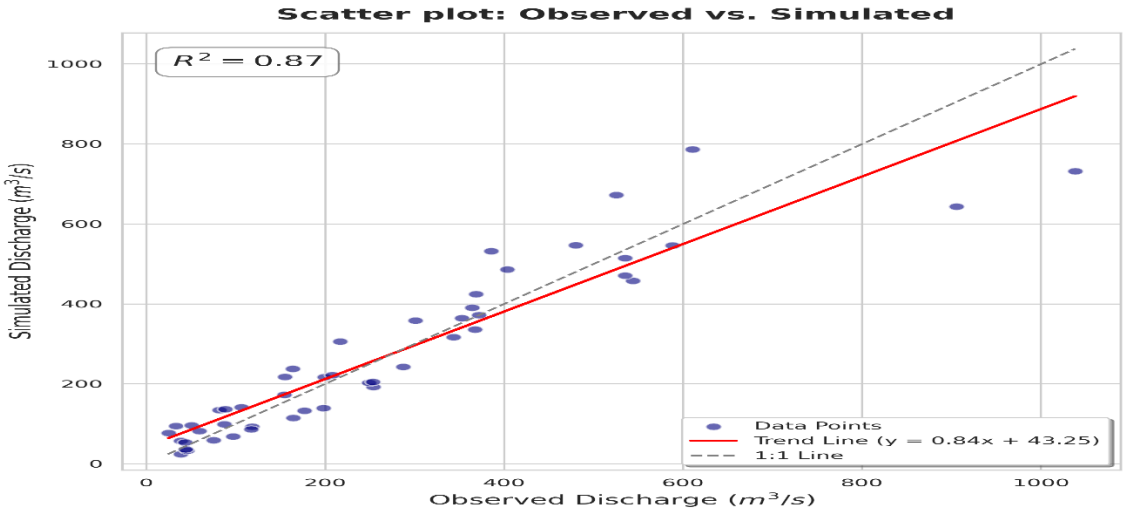

Figure 4-5: Scatter plot of Observed vs. Simulated monthly discharge

The statistical analysis yielded a Nash-Sutcliffe Efficiency (NSE) of 0.86, a Coefficient of Determination (R^2) of 0.87, and a Percent Bias ($PBIAS$) of -0.60%. The (R^2) value of 0.87 indicates a strong linear correlation, while the extremely low PBIAS confirms that the model accurately simulates the total water volume without significant bias. These results exceed

the recommended performance criteria for very good model performance (Moriasi et al., 2007).

4.3.3 Model Validation for Stream Flow

To verify the robustness of the calibrated parameters, model validation was conducted using an independent dataset from the years of 1999 and 2000. The hydrograph comparing observed and simulated discharge during the validation period is shown in Figure 4.6.

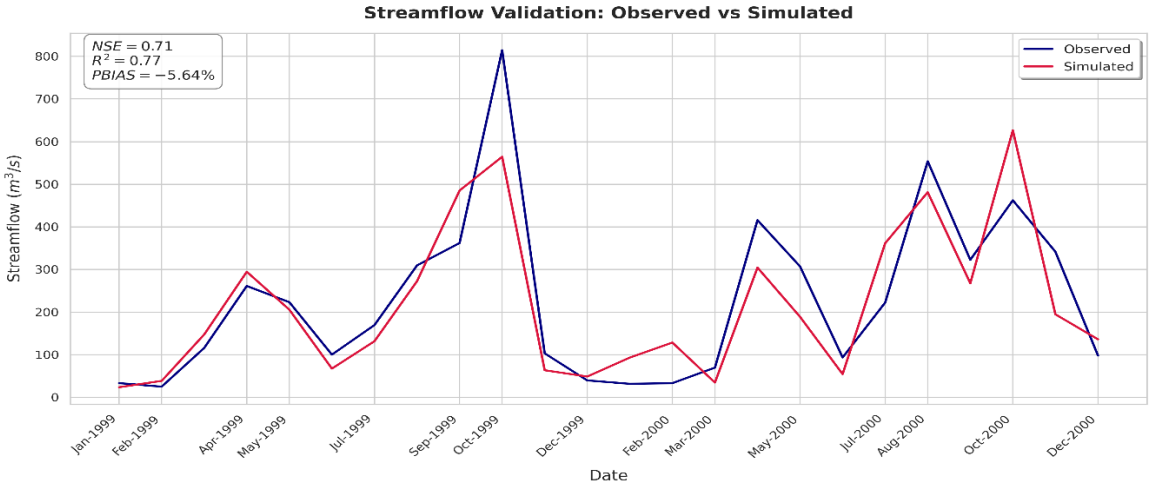

Figure 4-6: Observed vs. Simulated monthly streamflow hydrograph during validation (1999-2000).

The model maintained its performance during the validation period, achieving an (NSE) of 0.71 and an (R^2) of 0.77. The ($PBIAS$) increased slightly to -5.64% but remains well within the optimal range ($< \pm 10\%$), indicating a very accurate water balance simulation.

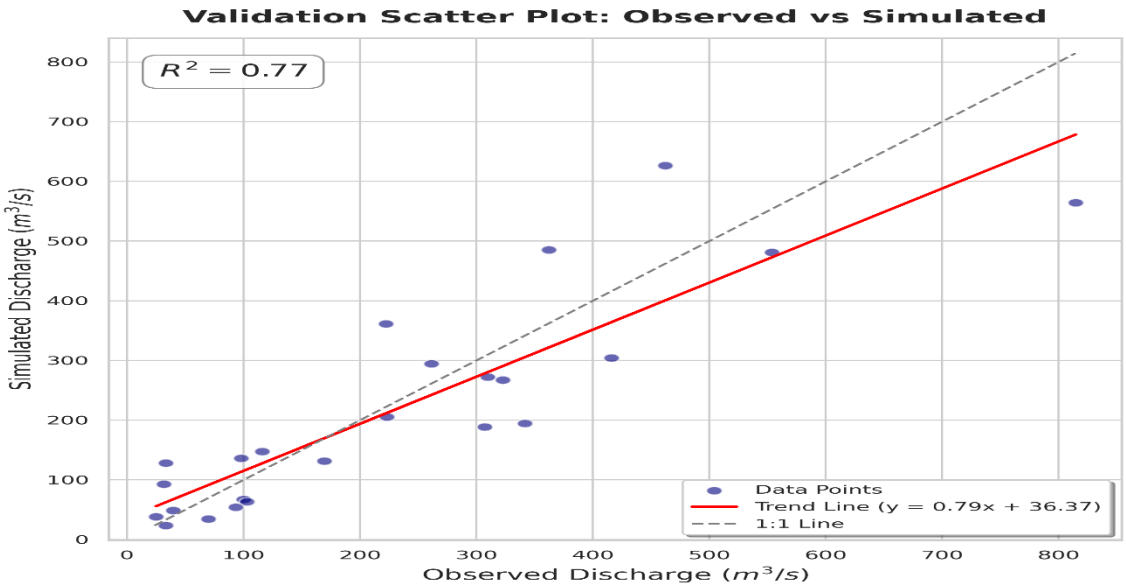

Figure 4-7: Scatter plot of Observed vs. Simulated monthly discharge during validation.

The scatter plot (Figure 4.7) confirms the strong linear relationship ($R^2 = 0.77$) between observed and simulated flows during the validation phase. The consistency of these results between calibration and validation demonstrates that the SWAT model is robust and capable of reliably simulating the hydrological processes of the region. Consequently, these calibrated parameters were deemed suitable for regionalization to the Humbo Weyne catchment.

4.4 Sediment Yield Modelling

Following the successful calibration of streamflow, the model was calibrated and validated for sediment yield. This step is crucial to ensure that the model accurately simulates erosion and sediment transport processes before transferring the parameters to the ungauged Humbo Weyne catchment.

4.4.1 Sensitivity Analysis

A global sensitivity analysis was conducted for sediment parameters using the SUFI-2 algorithm. Based on the methodology, 16 sediment-related parameters were tested to determine their influence on sediment yield simulation. The sensitivity was evaluated using t-stats and p-values.The results of the sediment sensitivity analysis are presented in Figure 4.8.

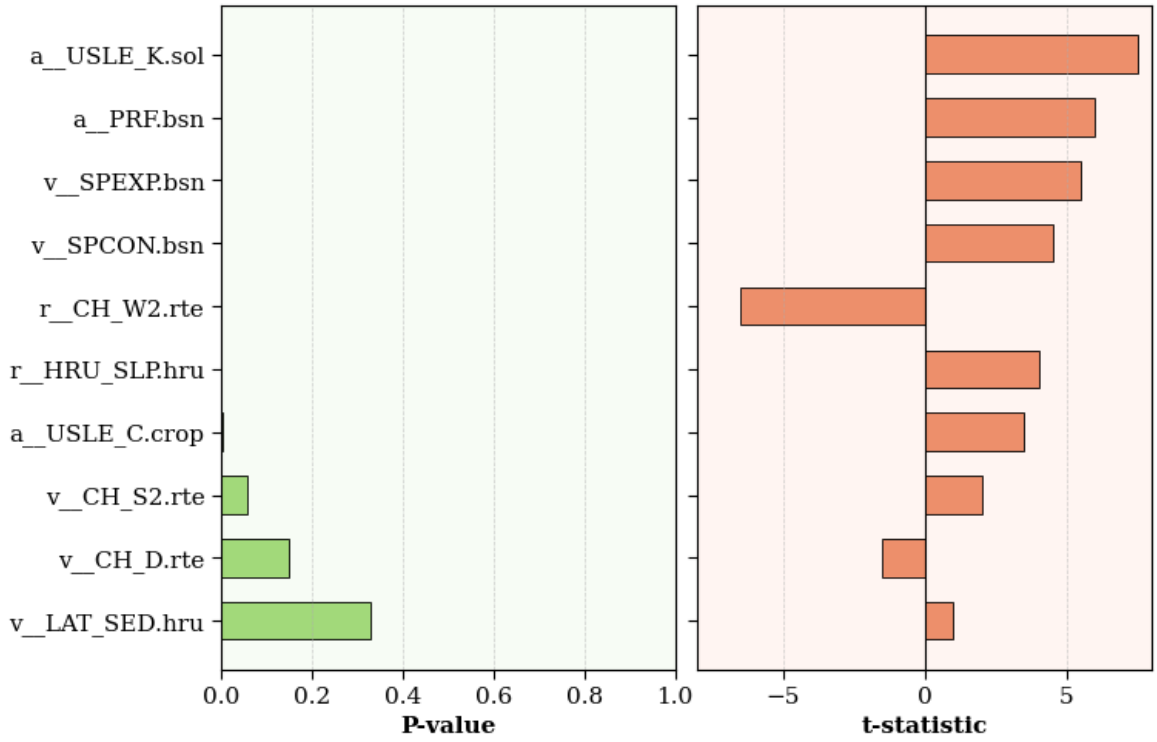

Figure 4-8: Global sensitivity analysis of sediment parameters for the Gode catchment.

As shown in Figure 4.9, the USLE Soil Erodibility Factor ($a\_USLE\_K.sol$) was identified as the most dominant parameter (t-stat > 7.5, p-value = 0.00). This indicates that the intrinsic susceptibility of the soil to detachment and transport is the primary driver of sediment yield in the catchment.

The Main Channel Width ($r\_CH\_W2.rte$) emerged as the second most sensitive parameter, with a high negative t-stat. This highlights the critical influence of channel geometry on sediment transport capacity and deposition processes.

Channel routing parameters also showed significant influence. The Peak Rate Adjustment Factor ($a\_PRF.bsn$) and the Exponent Parameter for Sediment Routing ($v\_SPEXP.bsn$) ranked third and fourth, respectively. This emphasizes the importance of peak flow characteristics and the non-linear relationships governing sediment re-entrainment in the river network.

Additionally, the Linear Parameter for Sediment Routing ($v\_SPCON.bsn$) and HRU Slope ($r\_HRU\_SLP.hru$) were found to be sensitive, further underlining the roles of channel sediment transport capacity and landscape topography. In contrast to previous iterations, lateral flow sediment parameters such as ($v\_LAT\_SED.hru$) showed lower sensitivity, suggesting channel and soil surface processes are the predominant factors.

4.4.2 Model Calibration for Sediment Yield

The model was calibrated for sediment yield using the observed sediment load data from the Gode gauging station. The calibration was performed on a monthly time step for the period of 1995 to 1998. The sensitive parameters identified were optimized to minimize the difference between observed and simulated sediment loads.

Table 4-1: Summary of calibrated sediment parameters for the Gode catchment.

S/no	Parameter Name	Description	Fitted Value	Min Value	Max Value
1	a__USLE_K.sol	USLE soil erodibility factor	0.17	0.00	0.20
2	r__CH_W2.rte	Average width of the main channel	0.14	0.00	0.20
3	a__PRF.bsn	Peak rate adjustment factor	0.10	0.00	0.20
4	v__SPEXP.bsn	Exponent parameter for channel sediment routing	1.35	1.00	1.50
5	v__SPCON.bsn	Linear parameter for channel sediment routing	0.004	0.00	0.001

6	r__HRU_SLP.hru	Average slope steepness	0.13	0.00	0.20
7	a__USLE_C.crop	USLE cover and management factor	0.14	0.00	0.20
8	v__CH_S2.rte	Average slope of main channel	0.004	0.001	10.00
9	v__CH_D.rte	Average depth of main channel	3.50	0.00	30.00
10	v__LAT_SED.hru	Sediment conc. in lateral flow	0.10	0.00	2.00

The calibration results showed a good agreement between the observed and simulated monthly sediment yields. Figure 4.9 illustrates the time series comparison, while Figure 4.10 shows the scatter plot correlation.

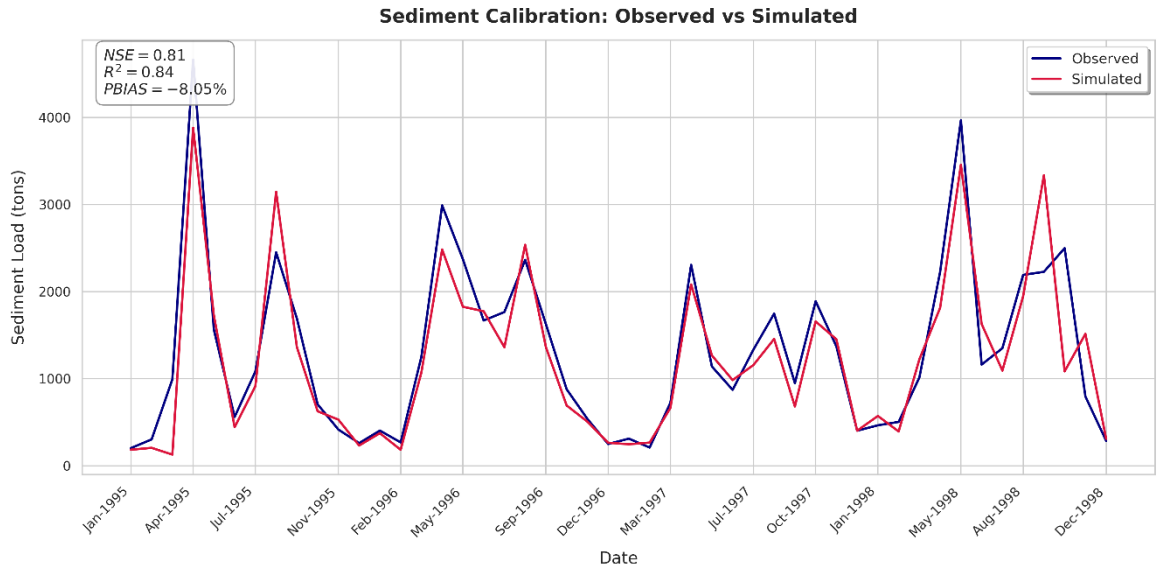

Figure 4-9: Observed vs. Simulated monthly sediment yield during calibration (1995–1998)

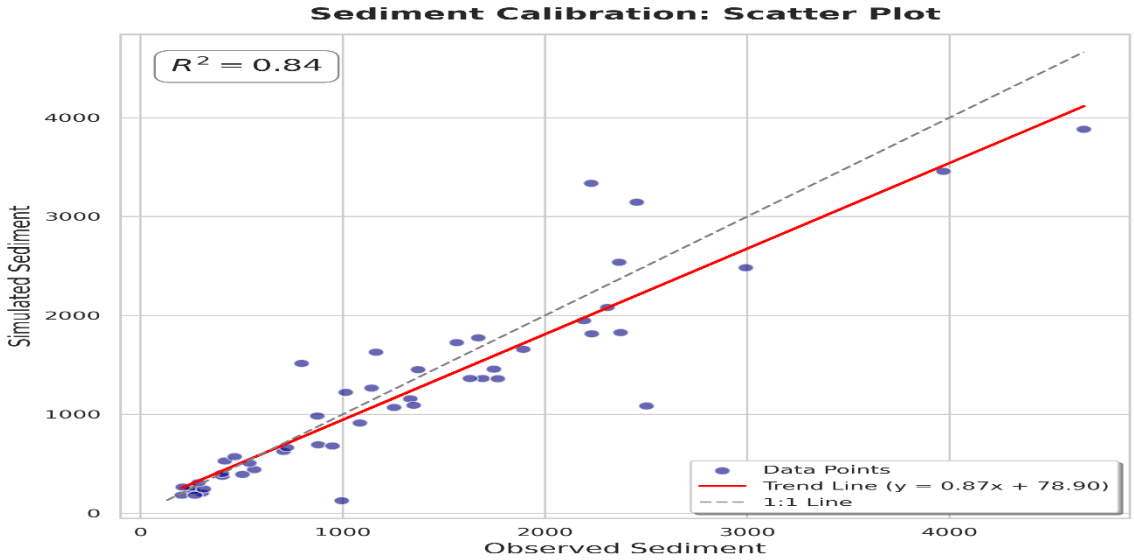

Figure 4-10: Scatter plot of observed vs. simulated sediment yield during calibration.

Statistical evaluation of the calibration period yielded an R^2 of 0.84, an NSE of 0.81, and a $PBIAS$ of -8.05%. The R^2 and NSE values indicate that the model successfully captures the timing and magnitude of sediment peaks. The negative $PBIAS$ indicates a slight overestimation bias, but it remains well within the acceptable range ($\pm 55\%$) for sediment simulations (Moriasi et al., 2007).

4.4.3 Model Validation for Sediment Yield

Model validation was carried out using an independent dataset from the years 1999 and 2000. The model was run using the parameters fixed during the calibration process without further adjustment.

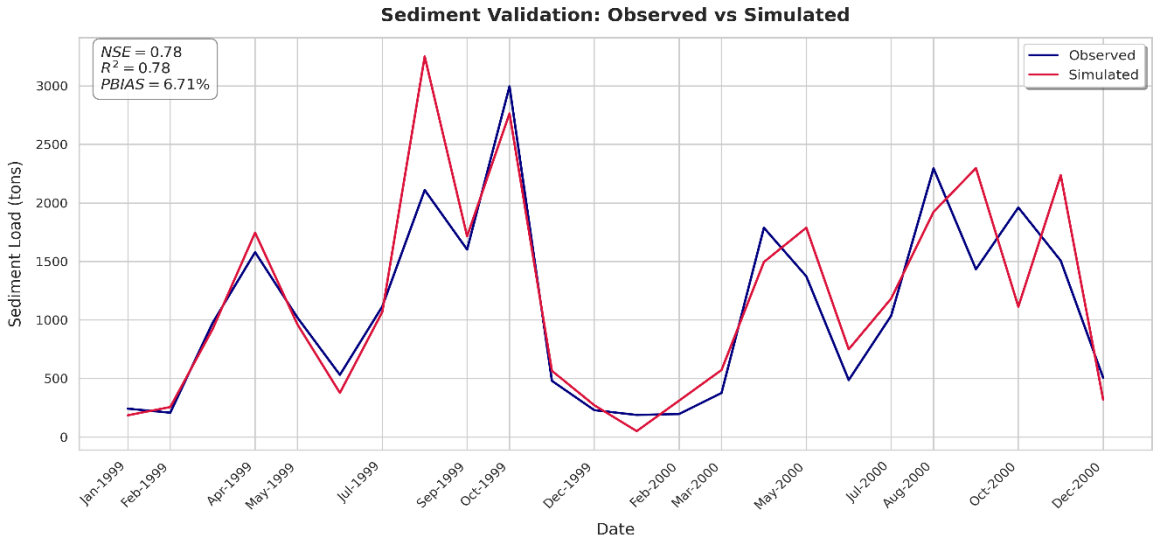

Figure 4-11: Observed vs. Simulated monthly sediment yield during validation (2000).

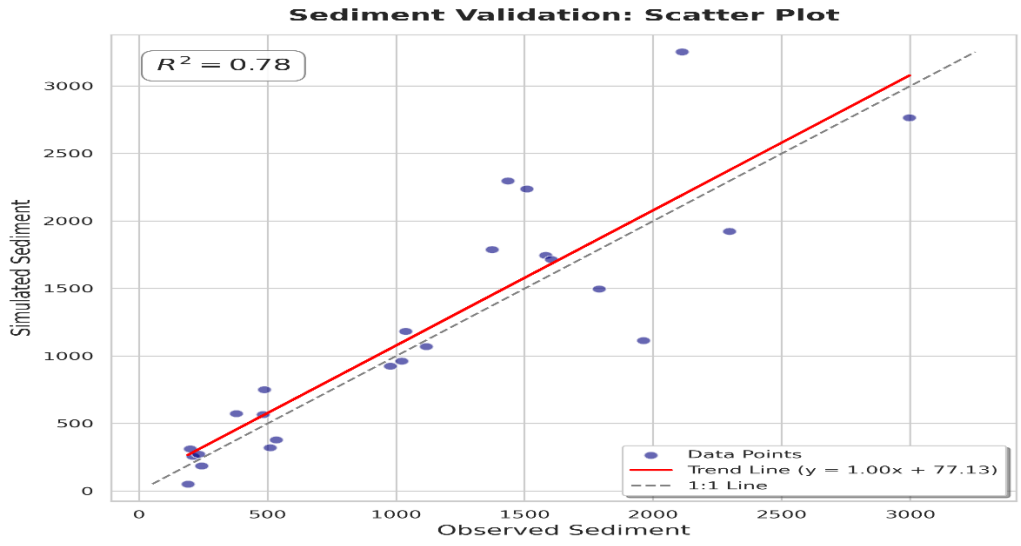

Figure 4-12: Scatter plot of observed vs. simulated sediment yield during validation.

The validation results demonstrated the model's robustness, achieving an NSE of 0.78 and an R^2 of 0.78. The $PBIAS$ was 6.71%, confirming that the model provides a reliable estimate of sediment transport in the catchment.

Based on these satisfactory performance metrics for both streamflow and sediment yield in the Gode catchment, the calibrated parameters were deemed scientifically valid for regionalization to the ungauged Humbo Weyne watershed.

4.5 Ungauged Catchment-Wide Sediment Yield

One of the primary objectives of this study was to quantify the annual sediment influx to the Humbo Weyne Dam. The optimized SWAT model, calibrated to the distinct semi-arid hydrology and erosion characteristics of the region, simulated an average annual sediment yield of 4.9 t/ha/yr across the 134,788.87-ha watershed. This corresponds to an estimated total influx of 660,000 tons of sediment delivered to the reservoir annually.

To evaluate the reliability of these findings, the simulated yield was compared with results from previous studies conducted in similar hydro-climatic zones of Ethiopia. As summarized in Table 4.7, the sediment yield of Humbo Weyne (4.9 t/ha/yr) is highly consistent with findings from the Central Rift Valley, particularly (Meshesha et al., 2011), who reported yields between 2.14 and 6.11 t/ha/yr for catchments with comparable Acacia woodland/shrubland cover. This similarity validates the model's ability to capture the transport-limited erosion dynamics typical of these dryland environments.

Table 4-2: Comparison of simulated sediment yield with other studies in the region

Watershed/Reservoir	Reference	Rainfall (mm)	Model Used	Sediment Yield (t/ha/yr)
Humbo Weyne	Current Study	~263	SWAT	4.9
Central Rift Valley	(Derege Tsegaye Meshesha et al., 2011)	500–1100	SWAT	2.14 – 6.11
Mormora	(W. G. Tenaw et al., 2024)	>1000	SWAT	8.54
Gumera (Lake Tana)	(M. Tenaw & Awulachew, 2009)	~1300	SWAT	11 – 22
Melkasa Dam	Bayisa (2019)	~800	SWAT	6.52
Fincha	(Ayana et al., 2012)	~1200	SWAT	14.5

However, notable differences exist when comparing this study to watersheds in the wetter Ethiopian highlands. For instance, (Tenaw et al., 2024) reported a higher yield of 8.54 t/ha/yr for the Mormora watershed. This discrepancy is physically justifiable given the climatic differences; Mormora receives significantly higher rainfall (>1000 mm), providing greater kinetic energy for soil detachment compared to the moisture-limited conditions of Humbo Weyne (~263 mm). Furthermore, highland catchments like Gumera (11–22 t/ha/yr) are heavily influenced by intensive tillage agriculture, whereas the Humbo Weyne watershed is dominated by pastoral rangelands where erosion is event-driven rather than tillage-induced.

Consequently, while the average yield of 4.9 t/ha/yr appears moderate, it remains a critical concern for the Humbo Weyne Dam, given that specific hotspot sub-basins (discussed in Section 4.8) generate yields exceeding 35 t/ha/yr, behaving similarly to the most degraded highland catchments.

4.6 Ungauged Catchment Spatial Variability and Erosion Hotspots

Although the watershed-wide sediment yield is moderate, the spatial analysis reveals substantial variability across the landscape. Sediment yields from individual routing units range from near-zero in the stable headwater areas to over 35 t/ha/yr in the escarpment region near the reservoir. To interpret this variability, the watershed was classified into erosion severity levels based on the FAO-SWALIM (Omuto et al., 2009) standards adapted for the Somali region. The distribution of these severity classes is summarized in Table 4.5.

Table 4-3: Erosion severity classification and areal extent in Humbo Weyne watershed

Sediment Interval (t/ha/yr)	Erosion Severity Class	Area Coverage (%)	Description
0 – 10	Low Risk	39.8	Tolerable erosion levels
10 – 20	Moderate Risk	19.9	Requires monitoring
20 – 30	High Risk	20.5	Requires intervention
30 – 35	Very High Risk	7.0	Critical priority
> 35	Severe Risk	12.8	Urgent rehabilitation needed

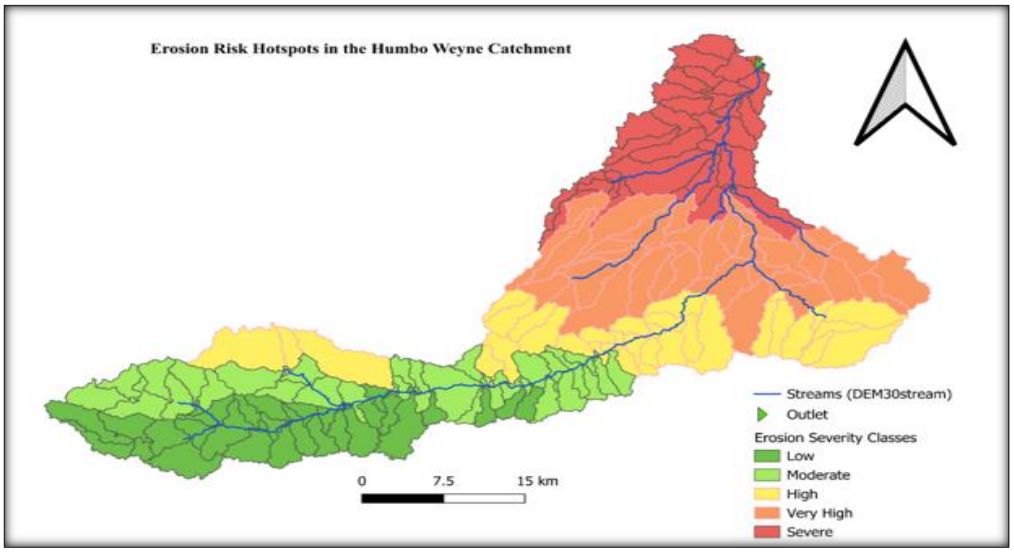

Figure 4-13: Erosion Severity Map of Humbo Weyne Catchment

Figure 4.13 (Erosion Severity Map) highlights a clear spatial dichotomy. Nearly 40% of the catchment, primarily the western and southwestern headwaters falls into the Low Risk category. These areas are characterized by flat terrain (slopes < 6.79%) and are dominated by agricultural land and pasture, which effectively limits runoff energy and minimizes sediment export.

In sharp contrast, the erosion hotspots are concentrated in the northeastern escarpment, located directly upstream of the dam. As shown in Table 4.8, the Very High and Severe risk categories combined cover 19.8% of the watershed. These critical zones are driven by the convergence of three aggravating physical factors:

1. **Steep Slopes:** Topography often exceeds 20%, generating high-velocity runoff.
2. **Bare Land Cover:** The area is dominated by barren or sparse vegetation classes, offering minimal canopy protection against raindrop impact.
3. **Weak Soil Types:** The soils are predominantly Inceptisols (63.5%) and Entisols (12.5%), both of which are structurally weak and highly prone to detachment.

4.6.1 Comparison of Spatial Patterns with Regional Studies

The spatial concentration of erosion observed in this study is consistent with patterns reported in other semi-arid Ethiopian catchments. For instance, (Daba et al., 2022) reported that 26.16% of the Awash Melkasa watershed was classified as erosion potential area, a figure comparable to the 19.8% critical hotspot area identified in Humbo Weyne. This suggests that in semi-arid environments, sediment yield is not generated uniformly but is often driven by specific distinct landscape units.

However, the extent of degradation in Humbo Weyne is notably less widespread than in the wetter highlands. (M. Tenaw & Awulachew, 2009) found that 72% of the Gumera watershed (Lake Tana basin) was erosion-prone. The lower proportion of severe erosion in Humbo Weyne (19.8% vs. 72%) confirms that while local degradation is intense (approaching 100 t/ha/yr in specific cells), the catchment as a whole is less active than the intensively cultivated highlands. This aligns with the global meta-analysis by (García-Ruiz et al., 2015), which characterizes semi-arid erosion as having moderate averages masked by extreme localized hotspots.

From a management perspective, the 19.8% of the watershed identified as hotspots (Very High to Severe risk) contributes disproportionately to the sediment delivery. Targeting these specific northeastern sub-basins for soil and water conservation measures such as hillside terracing and check dams would be the most cost-effective strategy to extend the operational lifespan of the Humbo Weyne reservoir.

CHAPTER FIVE: CONCLUSION AND RECOMMENDATIONS

This research was initiated to address a critical and fundamental gap in the water resource knowledge base for Somaliland: the complete absence of quantitative hydrological and sediment data for the vital, yet entirely ungauged, Humbo Weyne watershed. As highlighted in the problem statement, the Humbo Weyne Dam is currently in a state of dysfunction, with its designed storage capacity of 500,000 m^3 severely compromised by rapid siltation. Sustainable rehabilitation of this infrastructure and the planning of future water projects have historically been constrained by a reliance on assumptions rather than empirical evidence.

The primary objective of this study was, therefore, to conduct the first-ever comprehensive sediment yield modeling of the watershed using the SWAT model. By successfully employing a spatial proximity regionalization approach, this research has quantified the catchment's erosion dynamics, established the annual sediment budget entering the reservoir, and explicitly identified the high-risk source areas. These findings provide the essential scientific basis required to transition from reactive measures to proactive, data-driven management for the region's water security.

5.1 Conclusion

The sedimentation of the Humbo Weyne Dam presents a critical challenge to the water security of Hargeisa, exacerbated by the semi-arid climate and data scarcity characteristic of the Horn of Africa. This study successfully modeled the sediment yield of the Humbo Weyne watershed using the Soil and Water Assessment Tool (SWAT), employing a spatial proximity regionalization technique to overcome the lack of local gauging stations.

The study utilized a robust methodology, integrating high-resolution geospatial data (30m SRTM DEM, FAO soil map, and Copernicus Land Use/Land Cover) with bias-corrected CHIRPS satellite rainfall and ERA5 climate reanalysis data. The SWAT model was set up, calibrated, and validated on the hydrologically analogous Gode catchment in the Wabi Shebelle basin. Sensitivity analysis identified the SCS Runoff Curve Number (CN2) and the Soil Evaporation Compensation Factor (ESCO) as the most influential parameters governing the hydrological response, highlighting the dominance of surface runoff generation and evapotranspiration in the catchment's water balance. The model demonstrated reliable performance in the donor catchment, achieving a Nash-Sutcliffe Efficiency (NSE) of 0.86 for streamflow and 0.81 for sediment yield during the validation period, confirming its suitability for regionalization.

Following the transfer of optimized parameters to the ungauged Humbo Weyne watershed, the study simulated the hydrological and erosion dynamics over a 29-year period. The results indicate that the watershed generates an average annual sediment yield of 4.9 t/ha/yr. This translates to a substantial total annual sediment influx of approximately 660,000 tons into the Humbo Weyne reservoir. While this average yield falls within the Low Risk category typical of transport-limited semi-arid regions, the spatial analysis revealed significant variability. The majority of the catchment experiences low erosion rates; however, critical erosion hotspots were identified in the northeastern escarpment. These specific areas, covering approximately 19.8% of the watershed, are characterized by steep slopes, weak Inceptisol soils, and sparse vegetation, producing severe sediment yields exceeding 35 t/ha/yr. These findings confirm that the rapid siltation of the dam is driven by specific, identifiable high-risk zones rather than uniform degradation across the entire catchment. The study confirms that while the catchment is generally transport-limited due to low rainfall energy, the steep slopes and barren soils of the escarpment create localized zones of detachment-limited erosion that disproportionately threaten the reservoir.

5.2 Recommendations

Based on the findings of this study, the following recommendations are proposed to mitigate sedimentation and restore the dam's functionality:

1. **Prioritize the Northeastern Escarpment:** Conservation efforts must be targeted rather than broad. Immediate interventions such as stone bunds and hillside terracing as well as non-structural measures such as grazing management, afforestation, or conservation agriculture should be focused solely on the 19.8% of the watershed identified as Severe and Very High risk zones in the northeast.
2. **Sediment Trapping Upstream:** The construction of check dams (gabion or loose stone) in the primary gullies leading from the escarpment is critical to trapping coarse sediment before it reaches the reservoir.
3. **Hydro-Meteorological Monitoring:** Currently, Somaliland lacks a functional network of hydro-meteorological monitoring stations, which forces engineers to rely on estimation techniques like regionalization. To bridge this critical data gap, the Ministry of Water Resource Development must establish a permanent hydrometric station at the Humbo Wayne dam site. This station should be equipped to monitor daily streamflow inflow and suspended sediment concentration, providing the

essential ground-truth data required for the sustainable management of this dam and future national water infrastructure projects.

REFERENCES

Abbaspour, K. C. (2015). *SWATCalibration and Uncertainty Programs*.

Abbott, M. B., Bathurst, J. C., Cunge, J. A., O'Connell, P. E., & Rasmussen, J. (1986). An introduction to the European Hydrological System — Systeme Hydrologique Europeen, "SHE", 1: History and philosophy of a physically-based, distributed modelling system. *Journal of Hydrology*, *87*(1–2), 45–59. https://doi.org/10.1016/0022-1694(86)90114-9

Abdulkadir, G. (2017). *Assessment of Drought Recurrence in Somaliland: Causes, Impacts a*. https://www.iomcworld.com/open-access/assessment-of-drought-recurrence-in-somaliland-causes-impacts-and-mitigations-24423.html

Adnan, S., Aldefae, A. H., & Humaish, W. H. (2021). Soil erosion and the influenced factors: A review article. *IOP Conference Series: Materials Science and Engineering*, *1058*(1), 012041. https://doi.org/10.1088/1757-899X/1058/1/012041

Akoko, G., Le, T. H., Gomi, T., & Kato, T. (2021a). A Review of SWAT Model Application in Africa. *Water*, *13*(9), 1313. https://doi.org/10.3390/w13091313

Akoko, G., Le, T. H., Gomi, T., & Kato, T. (2021b). A Review of SWAT Model Application in Africa. *Water*, *13*(9), 1313. https://doi.org/10.3390/w13091313

Alasow, A. A., Hamed, M. M., Rady, M., Arab, M. A., Muhammad, M. K. I., & Shahid, S. (2024). *Spatiotemporal Analysis of Soil Moisture Drought in the Horn of Africa*. https://doi.org/10.21203/rs.3.rs-3953380/v1

Aleksey Y Sheshukov, Prasad Daggupati, Kyle R. Mankin, & Ming-Chieh Lee. (2011). (PDF) High spatial resolution soil data for watershed modeling: 1. Development of a SSURGO-ArcSWAT utility. *Journal of Natural & Environmental Sciences*, 15–24.

Allen, R. G. & Food and Agriculture Organization of the United Nations (Eds.). (1998). *Crop evapotranspiration: Guidelines for computing crop water requirements*. Food and Agriculture Organization of the United Nations.

Amini, A. (Ed.). (2018). *Sedimentation Engineering*. InTech. https://doi.org/10.5772/intechopen.68509

Annandale, G. W. (2005). Reservoir Sedimentation. In M. G. Anderson & J. J. McDonnell (Eds.), *Encyclopedia of Hydrological Sciences* (1st ed.). Wiley. https://doi.org/10.1002/0470848944.hsa086

Atulley, J., Kwaku, A. A., Owusu-Ansah, E. D., Ampofo, S., Jacob, A., & Nii, O. S. (2022). *Modeling the impact of past and future land cover changes on a reservoir catchment hydrology in Semi-arid, Africa*. https://doi.org/10.21203/rs.3.rs-1505575/v1

Ayana, A., Edossa, D., & Kositsakulchai, E. (2012). Simulation of Sediment Yield using SWAT Model in Fincha Watershed, Ethiopia. *Kasetsart Journal - Natural Science*, *046*, 283–297.

Ayele, G. T., Kuriqi, A., Jemberrie, M. A., Saia, S. M., Seka, A. M., Teshale, E. Z., Daba, M. H., Ahmad Bhat, S., Demissie, S. S., Jeong, J., & Melesse, A. M. (2021). Sediment Yield and Reservoir Sedimentation in Highly Dynamic Watersheds: The Case of Koga Reservoir, Ethiopia. *Water*, *13*(23), 3374. https://doi.org/10.3390/w13233374

Bagul, P. A., & Mohite, N. M. (2023). Sediment Yield Assessment of a Watershed Area Using SWAT. In M. S. Ranadive, B. B. Das, Y. A. Mehta, & R. Gupta (Eds.), *Recent Trends in Construction Technology and Management* (Vol. 260, pp. 415–424). Springer Nature Singapore. https://doi.org/10.1007/978-981-19-2145-2_32

Bakti, D., Zen, Z., Rosmayati, & Sabrina, R. (2024). The Impact of sedimentation of mud, sand and rubbish on sustainability of the Asahan River, North Sumatera. *IOP Conference Series: Earth and Environmental Science*, *1302*(1), 012069. https://doi.org/10.1088/1755-1315/1302/1/012069

Baxter, A. J., Verschuren, D., Peterse, F., Miralles, D. G., Martin-Jones, C. M., Maitituerdi, A., Van Der Meeren, T., Van Daele, M., Lane, C. S., Haug, G. H., Olago, D. O., & Sinninghe Damsté, J. S. (2023). Reversed Holocene temperature–moisture relationship in the Horn of Africa. *Nature*, *620*(7973), 336–343. https://doi.org/10.1038/s41586-023-06272-5

Beven, K. (2009). *Environmental modelling: An uncertain future? an introduction to techniques for uncertainty estimation in environmental prediction* (1. publ). Routledge.

Beven, K. J. (2012). *Rainfall-runoff modelling: The primer* (2nd ed). Wiley-Blackwell.

Bressiani, D. de A., Gassman, P. W., Fernandes, J. G., Garbossa, L. H. P., Srinivasan, R., Bonumá, N. B., & Mendiondo, E. M. (2015). Review of Soil and Water Assessment Tool (SWAT) applications in Brazil: Challenges and prospects. *International Journal of Agricultural and Biological Engineering*, *8*(3), 9–35. https://doi.org/10.25165/ijabe.v8i3.1765

Burnash, R. (1995). *The NWS River Forecast System-Catchment Modeling. In Singh, V., Ed., Computer Models of Watershed Hydrology, Water Resources Publication, Colorado, 311-366. - References—Scientific Research Publishing*. https://www.scirp.org/%28S%28351jmbntvnsjt1aadkozje%29%29/reference/referencespapers?referenceid=1227488

Cotter, A. S., Chaubey, I., Costello, T. A., Soerens, T. S., & Nelson, M. A. (2003). WATER QUALITY MODEL OUTPUT UNCERTAINTY AS AFFECTED BY SPATIAL RESOLUTION OF INPUT DATA[1]. *JAWRA Journal of the American Water Resources Association*, *39*(4), 977–986. https://doi.org/10.1111/j.1752-1688.2003.tb04420.x

D. N. Moriasi, J. G. Arnold, M. W. Van Liew, R. L. Bingner, R. D. Harmel, & T. L. Veith. (2007). Model Evaluation Guidelines for Systematic Quantification of Accuracy in Watershed Simulations. *Transactions of the ASABE*, *50*(3), 885–900. https://doi.org/10.13031/2013.23153

Daba, B. I., Demissie, T. A., & Tufa, F. G. (2022). *Sediment yield modeling in Awash Melkasa dam watershed, upper Awash River basin, Ethiopia*. https://link.springer.com/10.1007/s11600-022-00972-8

Daud, Y. (2022, May 25). *The Possible Impacts of Sedimentation to The Dam Structures Case Study Humbo-wayne Dam structure*.

Derege Tsegaye Meshesha, Atsushi Tsunekawa, Mitsuru Tsubo, & Nigussie Haregeweyn. (2011). Spatial analysis and semi-quantitative modeling of specific sediment yield in six catchments of the central rift valley of Ethiopia. *Journal of Food, Agriculture & Environment*, *9*(3 & 4), 784–792.

Do, X. K., Nguyen, T. H., Ngo, L. A., Felix, M. L., Jung, K., Faculty of Water Resources Engineering, Thuyloi University 175 Tay Son Street, Dong Da District, Hanoi, Vietnam, & Chungnam National University, Daejeon, Korea. (2022). Prediction of Reservoir Sedimentation in the Long Term Period Due to the Impact of Climate Change: A Case Study of Pleikrong Reservoir. *Journal of Disaster Research*, *17*(4), 552–560. https://doi.org/10.20965/jdr.2022.p0552

Dooge J., C. (1957). The rational method for estimating flood peaks. In *Engineering* (Vol. 184, Issue 1, p. 311). https://cir.nii.ac.jp/crid/1370576118798730626

Dooge, J. C. I. (1959). A general theory of the unit hydrograph. *Journal of Geophysical Research*, *64*(2), 241–256. https://doi.org/10.1029/JZ064i002p00241

Echogdali, F. Z., Boutaleb, S., Taia, S., Ouchchen, M., Id-Belqas, M., Kpan, R. B., Abioui, M., Aswathi, J., & Sajinkumar, K. S. (2022). Assessment of soil erosion risk in a semi-arid climate watershed using SWAT model: Case of Tata basin, South-East of Morocco. *Applied Water Science*, *12*(6), 137. https://doi.org/10.1007/s13201-022-01664-w

Foster, G. R., & Meyer, L. D. (1977). *SOIL EROSION AND SEDIMENTATION BY WATER -- AN OVERVIEW*. 1–13. https://trid.trb.org/View/79598

Garcia, X. (2023). Using the Soil and Water Assessment Tool (SWAT) to quantify the economic value of ecosystem services. *River*, *2*(2), 173–185. https://doi.org/10.1002/rvr2.47

García-Ruiz, J. M., Beguería, S., Nadal-Romero, E., González-Hidalgo, J. C., Lana-Renault, N., & Sanjuán, Y. (2015). A meta-analysis of soil erosion rates across the world. *Geomorphology*, *239*, 160–173. https://doi.org/10.1016/j.geomorph.2015.03.008

Gonzalez Rodriguez, L., McCallum, A., Kent, D., Rathnayaka, C., & Fairweather, H. (2023). A review of sedimentation rates in freshwater reservoirs: Recent changes and causative factors. *Aquatic Sciences*, *85*(2), 60. https://doi.org/10.1007/s00027-023-00960-0

Gurmu, Z., Ritzema, H., Fraiture, C., & Ayana, M. (2022). Sedimentation in small-scale irrigation schemes in Ethiopia: Its sources and management. *International Journal of Sediment Research*, *37*. https://doi.org/10.1016/j.ijsrc.2022.02.006

Han, X., Li, Y., Yu, W., & Feng, L. (2022). Attribution of the Extreme Drought in the Horn of Africa during Short-Rains of 2016 and Long-Rains of 2017. *Water*, *14*(3), 409. https://doi.org/10.3390/w14030409

Haun, S., Mouris, K., Schwindt, S., & Wieprecht, S. (2024, November 27). *Predicting global change effects on reservoir sedimentation*. https://doi.org/10.5194/egusphere-egu24-4113

Heber Green, W., & Ampt, G. A. (1911). Studies on Soil Phyics. *The Journal of Agricultural Science*, *4*(1), 1–24. https://doi.org/10.1017/S0021859600001441

Hilgert, S., Sotiri, K., & Fuchs, S. (2023). Review of methods of sediment detection in reservoirs. *International Journal of Sediment Research*, S1001627923000781. https://doi.org/10.1016/j.ijsrc.2023.12.004

Ines Gharnouki, Jalel Aouissi, Manel Mosbahi, & Sihem Benabdallah. (2024). Hydrological modelling using SWAT in a Complex Semi-Arid Watershed. *GSC Advanced Research and Reviews*, *21*(2), 238–247. https://doi.org/10.30574/gscarr.2024.21.2.0427

Islam, A., Chandra Das, B., Mahammad, S., Ghosh, P., Deb Barman, S., & Sarkar, B. (2021). Deforestation and its impact on sediment flux and channel morphodynamics of the Brahmani River Basin, India. In *Forest Resources Resilience and Conflicts* (pp. 377–415). Elsevier. https://doi.org/10.1016/B978-0-12-822931-6.00029-0

J. G. Arnold, D. N. Moriasi, P. W. Gassman, K. C. Abbaspour, M. J. White, R. Srinivasan, C. Santhi, R. D. Harmel, A. Van Griensven, M. W. Van Liew, N. Kannan, & M. K. Jha. (2012). SWAT: Model Use, Calibration, and Validation. *Transactions of the ASABE*, *55*(4), 1491–1508. https://doi.org/10.13031/2013.42256

J. K. Searcy & C. H. Hardison. (1960). Double Mass Curves. Manual of hydrology Part 1. General Surface Water Techniques," r 1541-B., 1960. - References—Scientific Research Publishing. *US Geological Survey, Water-Supply Paper*. https://www.scirp.org/reference/referencespapers?referenceid=396974

Jaiswal, A., Ahmad, Z., & Mishra, S. K. (2024, November 27). *Navigating reservoir sedimentation through hydro-suction*. https://doi.org/10.5194/egusphere-egu24-4253

Janjić, J., & Tadić, L. (2023). Fields of Application of SWAT Hydrological Model—A Review. *Earth*, *4*(2), 331–344. https://doi.org/10.3390/earth4020018

Jiménez, S., Juárez-Ramírez, R., Castillo, V. H., & Tapia Armenta, J. J. (2018). A Model for Providing Affective Feedback. In S. Jiménez, R. Juárez-Ramírez, V. H. Castillo, & J. J. Tapia Armenta, *Affective Feedback in Intelligent Tutoring Systems* (pp. 27–46). Springer International Publishing. https://doi.org/10.1007/978-3-319-93197-5_3

Jordan, S., Quinn, J., Zaniolo, M., Giuliani, M., & Castelletti, A. (2022). Advancing reservoir operations modelling in SWAT to reduce socio-ecological tradeoffs. *Environmental Modelling & Software*, *157*, 105527. https://doi.org/10.1016/j.envsoft.2022.105527

Khalid, K., Ali, M. F., & Abd Rahman, N. F. (2015). The Development and Application of Malaysian Soil Taxonomy in SWAT Watershed Model. In S. H. Abu Bakar, W. Tahir, M. Ab. Wahid, S. R. Mohd Nasir, & R. Hassan (Eds.), *ISFRAM 2014* (pp. 77–88). Springer Singapore. https://doi.org/10.1007/978-981-287-365-1_7

Koppa, A., Keune, J., MacLeod, D. A., Singer, M., & Miralles, D. G. (2022, March 27). *Unraveling the Origin of Rainfall over Horn of Africa Drylands*. https://doi.org/10.5194/egusphere-egu22-5330

Koycegiz, C., & Buyukyildiz, M. (2019). Calibration of SWAT and Two Data-Driven Models for a Data-Scarce Mountainous Headwater in Semi-Arid Konya Closed Basin. *Water*, *11*(1), 147. https://doi.org/10.3390/w11010147

Krause, P., Boyle, D. P., & Bäse, F. (2005). Comparison of different efficiency criteria for hydrological model assessment. *Advances in Geosciences*, *5*, 89–97. https://doi.org/10.5194/adgeo-5-89-2005

Kuana, L. A., Almeida, A. S., Mercuri, E. G. F., & Noe, S. M. (2023). *Regionalization of GR4J model parameters for river flow prediction in Paraná, Brazil*. https://doi.org/10.5194/egusphere-2023-1755

Lee, J., Han, J., Lee, S., Kim, J., Na, E. H., Engel, B., & Lim, K. J. (2024). Enhancing Sustainability in Watershed Management: Spatiotemporal Assessment of Baseflow Alpha Factor in SWAT. *Sustainability*, *16*(21), 9189. https://doi.org/10.3390/su16219189

Li, H., Yu, C., Qin, B., Li, Y., Jin, J., Luo, L., Wu, Z., Shi, K., & Zhu, G. (2022). Modeling the Effects of Climate Change and Land Use/Land Cover Change on Sediment Yield in a Large Reservoir Basin in the East Asian Monsoonal Region. *Water*, *14*(15), 2346. https://doi.org/10.3390/w14152346

Liu, L., Cao, X., Li, S., & Jie, N. (2024). A 31-year (1990–2020) global gridded population dataset generated by cluster analysis and statistical learning. *Scientific Data*, *11*(1), 124. https://doi.org/10.1038/s41597-024-02913-0

Maskey, S. (2022). Introduction. In *Catchment Hydrological Modelling* (pp. 1–16). Elsevier. https://doi.org/10.1016/B978-0-12-818337-3.00001-5

Megnounif, A., Terfous, A., Ghenaim, A., & Poulet, J.-B. (2007). Key processes influencing erosion and sediment transport in a semi-arid Mediterranean area: The Upper Tafna catchment, Algeria / *Processus clefs influençant l'érosion et le transport des sédiments dans une région semi-aride Méditerranéenne: le bassin versant de la Haute Tafna, Algérie*. *Hydrological Sciences Journal*, *52*(6), 1271–1284. https://doi.org/10.1623/hysj.52.6.1271

Mekonnen, Y. A., Mengistu, T. D., Asitatikie, A. N., & Kumilachew, Y. W. (2022). Evaluation of reservoir sedimentation using bathymetry survey: A case study on Adebra night storage reservoir, Ethiopia. *Applied Water Science*, *12*(12), 269. https://doi.org/10.1007/s13201-022-01787-0

Meyer, L. D. (1986). Erosion processes and sediment properties for agricultural cropland. In *Hillslope Processes*. Routledge.

Mikos, M. (2004). Sediment Transport. In J. H. Lehr & J. Keeley (Eds.), *Water Encyclopedia* (1st ed., pp. 417–421). Wiley. https://doi.org/10.1002/047147844X.sw858

Moges, E., Demissie, Y., Larsen, L., & Yassin, F. (2020). Review: Sources of Hydrological Model Uncertainties and Advances in Their Analysis. *Water*, *13*(1), 28. https://doi.org/10.3390/w13010028

Mologni, C., Revel, M., Chaumillon, E., Malet, E., Coulombier, T., Sabatier, P., Brigode, P., Hervé, G., Develle, A.-L., Schenini, L., Messous, M., Davtian, G., Carré, A., Bosch, D., Volto, N., Ménard, C., Khalidi, L., & Arnaud, F. (2024). 50-year seasonal variability in East African droughts and floods recorded in central Afar lake sediments (Ethiopia) and their connections with the El Niño–Southern Oscillation. *Climate of the Past*, *20*(8), 1837–1860. https://doi.org/10.5194/cp-20-1837-2024

Mouris, K., Schwindt, S., Pesci, M. H., Wieprecht, S., & Haun, S. (2023). An interdisciplinary model chain quantifies the footprint of global change on reservoir sedimentation. *Scientific Reports*, *13*(1), 20160. https://doi.org/10.1038/s41598-023-47501-1

Mueller, E. N., Güntner, A., Francke, T., & Mamede, G. (2010). Modelling sediment export, retention and reservoir sedimentation in drylands with the WASA-SED model. *Geoscientific Model Development*, *3*(1), 275–291. https://doi.org/10.5194/gmd-3-275-2010

Muktadir, M. A., Koppa, A., Claessen, J., MacLeod, D. A., Singer, M., & Miralles, D. G. (2022, March 28). *Links between land cover change and climate in the Horn of Africa*. https://doi.org/10.5194/egusphere-egu22-10577

Neitsch, S. L., Arnold, J. G., Kiniry, J. R., & Williams, J. r. (2009). *SWAT theoretical documentation version 2009* (Technical Report No. 406). Texs water resource institute. https://swat.tamu.edu/media/99192/swat2009-theory.pdf

Omer, M. A. (2024). Climate variability and livelihood in Somaliland: A review of the impacts, gaps, and ways forward. *Cogent Social Sciences*, *Volume 10*, 2299108. https://doi.org/10.1080/23311886.2023.2299108

Omuto, C. T., Vargas, R. R., & Paron, P. (2009). *SOIL EROSION AND SEDIMENTATION MODELLING AND MONITORING OF THE AREAS BETWEEN RIVERS JUBA AND SHABELLE IN SOUTHERN SOMALIA*. FA0-SWALIM. https://www.faoswalim.org/resources/site_files/L-16%20Soil%20Erosion%20and%20Sedimentation%20Modelling.pdf

P. W. Gassman, M. R. Reyes, C. H. Green, & J. G. Arnold. (2007). The Soil and Water Assessment Tool: Historical Development, Applications, and Future Research Directions. *Transactions of the ASABE*, *50*(4), 1211–1250. https://doi.org/10.13031/2013.23637

Perera, D., Williams, S., & Smakhtin, V. (2022). Present and Future Losses of Storage in Large Reservoirs Due to Sedimentation: A Country-Wise Global Assessment. *Sustainability*, *15*(1), 219. https://doi.org/10.3390/su15010219

R. Williams, J., & D. Berndt, H. (1977). Sediment Yield Prediction Based on Watershed Hydrology. *Transactions of the ASAE*, *20*(6), 1100–1104. https://doi.org/10.13031/2013.35710

Raes, D., Willems, P., & Gbaguidi, F. (2006). *RAINBOW - a software package for hydrometeorological frequency analysis and testing the homogeneity of historical data sets*.

Rallison, R. E., & Miller, N. C. (1982). *Past, present, and future SCS runoff procedure*.

Randle, T. J., Collins, K. L., & Gray, J. R. (2013). Avoiding The Inevitable? Capacity Loss From Reservoir Sedimentation: Reservoir Sustainability Workshop; Lakewood, Colorado, 10–12 July 2012. *Eos, Transactions American Geophysical Union*, *94*(1), 4–4. https://doi.org/10.1002/2013EO010008

SAAB TV (Director). (2018, February 14). *Mareyihii Hore Ee wakaalada Biyaha Hargaysa Oo Shaaciyay Inuu Mashrucii Xumbo Wayne Fashilmay* [Video recording]. https://www.youtube.com/watch?v=165qafcNpDk

Sabale, R. S., Londhe, S., & Jose, M. K. (2023). Reservoir Sedimentation Analysis Using SWAT Model. In P. V. Timbadiya, P. L. Patel, V. P. Singh, & P. J. Sharma (Eds.), *Hydrology and Hydrologic Modelling* (Vol. 312, pp. 167–180). Springer Nature Singapore. https://doi.org/10.1007/978-981-19-9147-9_12

Setegn, S. G., Srinivasan, R., & Dargahi, B. (2008). Hydrological Modelling in the Lake Tana Basin, Ethiopia Using SWAT Model. *The Open Hydrology Journal*, *2*(1), 49–62. https://doi.org/10.2174/1874378100802010049

Shahin, M. (2007). Erosion and sedimentation in drainage basins and in storage reservoirs. In V. P. Singh, M. Anderson, L. Bengtsson, J. F. Cruise, U. C. Kothyari, S. E. Serrano, D. Stephenson, & W. G. Strupczewski (Eds.), *Water Resources and Hydrometeorology of the Arab Region* (Vol. 59, pp. 333–367). Springer Netherlands. https://doi.org/10.1007/1-4020-5414-9_8

Shrivastava, N., & Rai, A. K. (2023). Assessment of Sediment Hazard and Associated Measurement. In M. Pandey, H. Azamathulla, & J. H. Pu (Eds.), *River Dynamics and Flood Hazards* (pp. 17–42). Springer Nature Singapore. https://doi.org/10.1007/978-981-19-7100-6_2

Somaliland Channel (Director). (2017, April 25). *Barmaamijka Dhaamka Xumbo weyne Xabaal iyo Ninkeed loo kala teg* [Video recording]. https://www.youtube.com/watch?v=qQe-4YDNGyg

Sophiya, M., & Updhayaya, C. (2023). Assessment of Reservoir Sedimentation Using RS and GIS Techniques: A Case Study of Singda Dam, Manipur, India. *SAMRIDDHI : A Journal of Physical Sciences, Engineering and Technology*, *15*(02), 263–270. https://doi.org/10.18090/samriddhi.v15i02.13

Staff. (2018, November 16). *Exclusive Interview with Wassim Haroun of CONSER – (Part 1 – Xumboweyne Dam).* Somaliland Chronicle. https://somalilandchronicle.com/2018/11/16/exclusive-interview-with-wassim-haroun-of-conser-part-1-xumboweyne-dam/

Steinschneider, S., Yang, Y.-C. E., & Brown, C. (2015). Combining regression and spatial proximity for catchment model regionalization: A comparative study. *Hydrological Sciences Journal*, *60*(6), 1026–1043. https://doi.org/10.1080/02626667.2014.899701

Tang, X., Zhang, J., Wang, G., Jin, J., Liu, C., Liu, Y., He, R., & Bao, Z. (2021). Uncertainty Analysis of SWAT Modeling in the Lancang River Basin Using Four Different Algorithms. *Water, 13*(3), 341. https://doi.org/10.3390/w13030341

Tenaw, M., & Awulachew, S. B. (2009). *Soil and Water Assessment Tool (SWAT)-based runoff and sediment yield modeling: A case of the Gumera Watershed in Lake Tana Sub Basin*. https://hdl.handle.net/10568/38174

Tenaw, W. G., Tadesse, K. B., & Kerebih, M. S. (2024). Estimation of Sediment Yield and Evaluation of Management Options in the Watershed Using SWAT Model. *Air, Soil and Water Research, 17*, 11786221241284461. https://doi.org/10.1177/11786221241284461

Tessema, S. M. (2011). *Hydrological modeling as a tool for sustainable water resources management: A case study of the Awash River Basin*. https://urn.kb.se/resolve?urn=urn:nbn:se:kth:diva-33617

Tessema, Y. M., Zimale, F. A., & Kebedew, M. G. (2024). Understanding sedimentation trends to enhance sustainable reservoir management in the Angereb reservoir, Upper Blue Nile Basin, Ethiopia. *Frontiers in Water, 6*, 1387915. https://doi.org/10.3389/frwa.2024.1387915

Tsige, M. G., & Malcherek, A. (2024). *Deriving a Soil Loss Equation for Sediment Yield Estimation*. https://doi.org/10.31224/4010

Tundu, C., Tumbare, M. J., & Kileshye Onema, J.-M. (2018). Sedimentation and Its Impacts/Effects on River System and Reservoir Water Quality: Case Study of Mazowe Catchment, Zimbabwe. *Proceedings of the International Association of Hydrological Sciences*, *377*, 57–66. https://doi.org/10.5194/piahs-377-57-2018

United States Soil Conservation, S. (1972). *SCS National Engineering Handbook, Section 4: Hydrology*. The Service.

Wagener, T., & Gupta, H. V. (2005). Model identification for hydrological forecasting under uncertainty. *Stochastic Environmental Research and Risk Assessment*, *19*(6), 378–387. https://doi.org/10.1007/s00477-005-0006-5

Wharton, G., Mohajeri, S. H., & Righetti, M. (2017). The pernicious problem of streambed colmation: A multi-disciplinary reflection on the mechanisms, causes, impacts, and management challenges. *WIREs Water*, *4*(5), e1231. https://doi.org/10.1002/wat2.1231

Wheater, H., Sorooshian, S., & Sharma, K. D. (Eds.). (2007). *Hydrological Modelling in Arid and Semi-Arid Areas* (1st ed.). Cambridge University Press. https://doi.org/10.1017/CBO9780511535734

Williams, J. R., & Hann, R. W. (1973). *HYMO: problem oriented computer language for hydrologic modeling*. https://www.tucson.ars.ag.gov/unit/publications/PDFfiles/964.pdf

Yimam, M. (2023). A Review on Climate Change and Hydrological Models. *Advances in Physics Theories and Applications*. https://doi.org/10.7176/APTA/87-01

Yuan, Y., & Koropeckyj-Cox, L. (2022). SWAT model application for evaluating agricultural conservation practice effectiveness in reducing phosphorous loss from the

Western Lake Erie Basin. *Journal of Environmental Management*, *302*, 114000. https://doi.org/10.1016/j.jenvman.2021.114000

APPENDIX

Appendix A: Data Quality Assessment

Appendix A1: Homogeneity test result for Rainfall stations

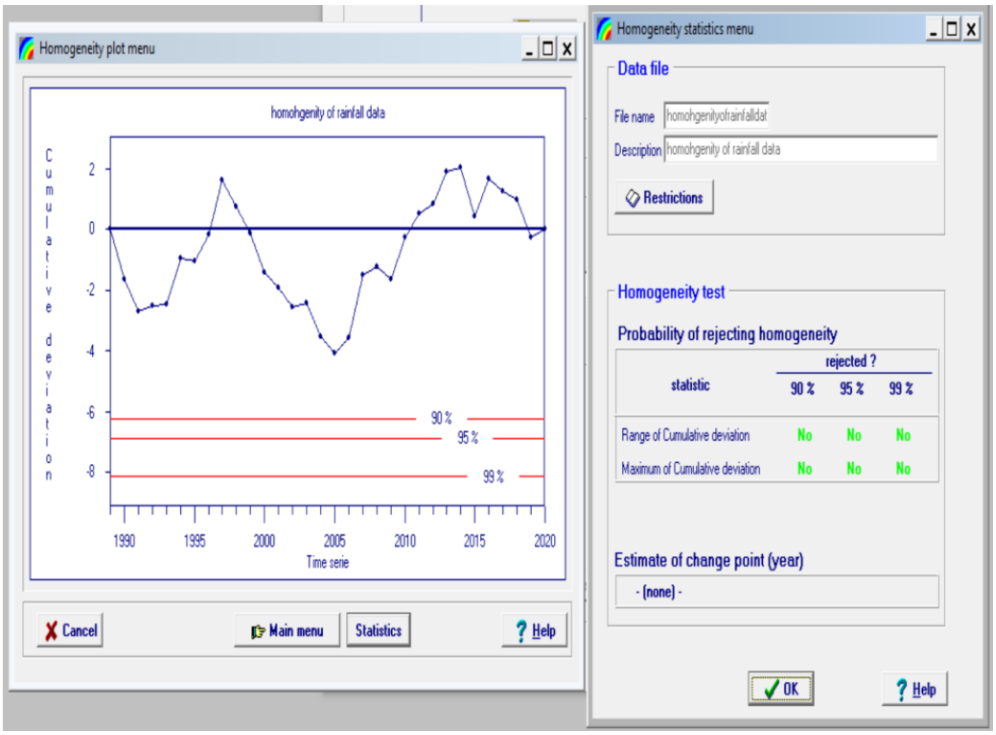

Appendix A2: Homogeneity test result for Hydrological data

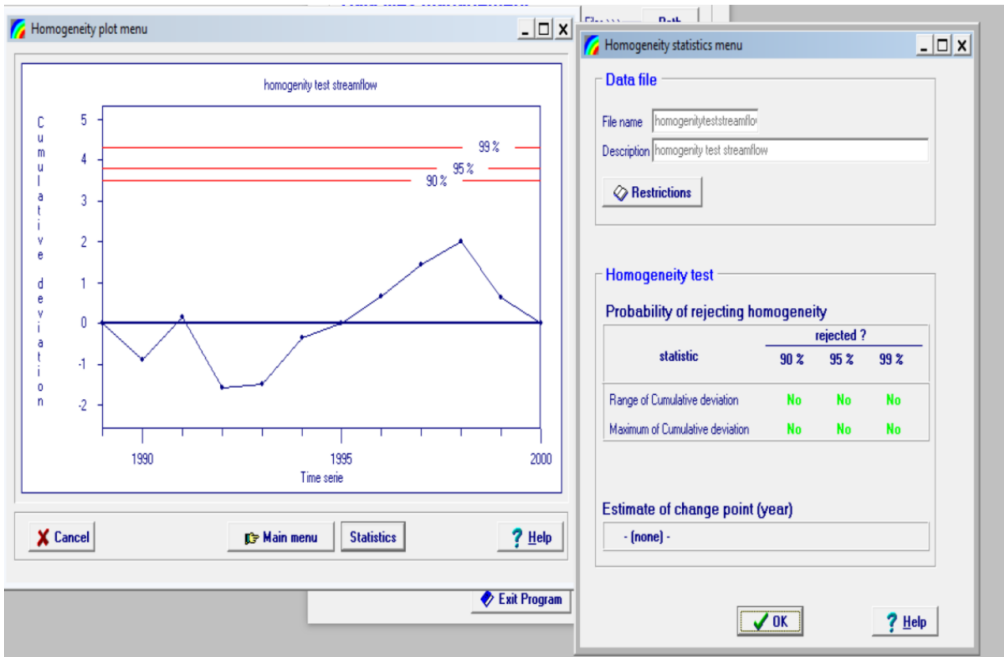

Appendix B: Annual Rainfall Totals

Appendix B1: Annual Rainfall Totals for Gauged Catchment Stations

Year	Ginir Station	Gode Station	Harar Station
1998	952.1	258.7	640.1
1999	725.9	196.8	888.0
2000	675.7	303.5	552.1

Appendix B2: Annual Rainfall Totals for Ungauged Catchment Stations

Year	Aburin	Botor	Dararweyne	Dhubato	Geed Deeble	Hargeisa
1995	136.0	322.6	94.3	356.9	120.6	327.8
1996	238.6	183.9	71.1	343.7	41.2	264.6
1997	325.7	166.4	74.5	522.5	81.1	525.4
1998	125.8	157.3	15.2	151.8	83.1	256.9
1999	123.5	166.6	11.4	195.1	80.2	165.1
2000	97.0	209.0	72.3	230.0	50.7	150.1
2001	93.4	129.6	53.1	61.1	46.6	91.1
2002	163.9	150.1	13.4	120.5	111.2	146.1
2003	23.4	31.5	51.9	160.4	218.2	317.8
2004	140.7	179.9	39.1	181.2	109.8	180.3
2005	212.1	434.8	81.3	315.3	193.4	314.0
2006	152.8	234.4	110.0	160.7	168.0	473.5
2007	256.5	229.8	87.3	392.5	162.3	574.7
2008	239.0	73.2	6.4	345.2	85.5	380.0
2009	216.0	234.6	54.6	360.7	146.5	309.5
2010	391.0	282.8	122.1	449.7	167.9	521.0
2011	357.6	150.5	115.3	315.5	171.9	398.5

Year	Aburin	Botor	Dararweyne	Dhubato	Geed Deeble	Hargeisa
2012	223.9	262.5	60.6	298.0	189.7	380.8
2013	419.5	392.7	87.5	503.0	202.7	576.0
2014	356.5	245.8	191.5	285.5	106.5	423.5
2015	148.5	178.1	111.3	183.0	90.0	244.5
2016	399.5	517.0	105.5	231.5	307.3	434.0
2017	405.5	376.5	194.0	358.5	141.2	241.0
2018	382.0	350.0	103.3	572.0	117.8	374.0
2019	303.5	494.0	275.5	521.0	83.7	523.0
2020	416.0	259.0	333.0	489.0	554.5	606.0
2021	422.5	430.0	267.5	559.5	496.0	753.5
2022	324.0	261.0	215.0	261.0	123.0	282.0
2023	603.5	278.5	325.5	729.5	548.0	644.5
2024	712.5	609.0	187.0	733.0	377.0	952.0

Appendix C: Soil Database Tables

Appendix C1: List of Soils and their User Codes in the Gode Watershed

S.No	User Code (Grid Value)	Soil Name (SWAT Code)	Texture Class
1	1	Af14-3c-1	CLAY_LOAM
2	9	Bd30-2-3c-9	CLAY_LOAM
3	26	Be9-3c-26	CLAY
4	31	Bh12-3c-31	CLAY_LOAM
5	48	Fp9-3a-48	CLAY
6	101	Jc21-3a-101	CLAY
7	102	Jc21-3a-102	CLAY
8	154	Ne10-3b-154	SANDY_CLAY_LOAM
9	159	Ne15-3c-159	SANDY_CLAY_LOAM
10	201	Rc18-3b-201	CLAY
11	204	Rc19-bc-204	CLAY_LOAM
12	207	Rc2-3c-207	LOAM
13	208	Rc20-3a-208	CLAY_LOAM
14	210	Rc20-ab-210	CLAY
15	211	Rc21-2c-211	CLAY
16	229	Rd2-2c-229	SANDY_LOAM
17	240	Re48-2a-240	SANDY_LOAM
18	246	Re59-2c-246	LOAM
19	283	Vp1-3a-283	CLAY
20	306	Xh15-3a-306	SANDY_LOAM
21	348	Yh16-2-3c-348	CLAY
22	356	Yh19-2a-356	CLAY

S.No	User Code (Grid Value)	Soil Name (SWAT Code)	Texture Class
23	358	Yh21-2ab-358	CLAY

Appendix C2: Physicochemical Properties of Soils in the Gode Watershed

Soil Name	Hyd Grp	Max Depth (mm)	BD (g/cm³)	AWC (mm/mm)	K-sat (mm/hr)	Org Carb (%)	Clay (%)	Silt (%)	Sand (%)	USLE_K
Af14-3c-1	C	750	1.2	0.144	13.87	1.6	38	26	36	0.25
Bd30-2-3c-9	C	560	1.1	0.092	20.22	2.3	28	31	41	0.26
Be9-3c-26	C	930	1.1	0.17	23.56	0.7	43	28	29	0.26
Bh12-3c-31	C	580	1.1	0.085	22.04	2.8	36	26	37	0.27
Fp9-3a-48	C	720	1.2	0.124	14.41	1.3	42	25	32	0.21
Jc21-3a-101	C	700	1.2	0.1	16.48	1.2	35	33	32	0.24
Jc21-3a-102	C	700	1.2	0.1	16.48	1.2	35	33	32	0.24
Ne10-3b-154	B	850	1.4	0.143	27.65	0.6	21	18	61	0.24
Ne15-3c-159	B	910	1.3	0.144	20.35	1	21	19	60	0.27
Rc18-3b-201	C	1200	1.2	0.141	15	0.8	39	24	37	0.22
Rc19-bc-204	C	1000	1.3	0.144	8.84	0.6	45	25	30	0.25
Rc2-3c-207	B	650	1.3	0.175	9.92	2.7	22	31	46	0.28
Rc20-3a-208	C	900	1.2	0.144	13.87	1.6	38	26	36	0.25
Rc20-ab-210	C	900	1.3	0.134	4.88	0.9	50	26	24	0.22
Rc21-2c-211	C	900	1.2	0.124	14.41	1.3	42	25	32	0.21
Rd2-2c-229	A	450	1.4	0.128	38.6	0.4	16	17	67	0.21
Re48-2a-240	A	1340	1.4	0.119	43.1	0.4	16	10	74	0.18
Re59-2c-246	B	1080	1.3	0.175	9.92	2.7	22	31	46	0.28
Vp1-3a-283	D	1000	1.1	0.15	5.2	0.9	62	23	15	0.21
Xh15-3a-306	A	930	1.5	0.13	34	0.5	17	12	71	0.17

Soil Name	Hyd Grp	Max Depth (mm)	BD (g/cm³)	AWC (mm/mm)	K-sat (mm/hr)	Org Carb (%)	Clay (%)	Silt (%)	Sand (%)	USLE_K
Yh16-2-3c-348	C	700	1.1	0.14	19.3	0.7	31	29	40	0.28
Yh19-2a-356	D	750	1.1	0.14	3.5	1.2	58	26	16	0.23
Yh21-2ab-358	C	750	1.1	0.12	5.1	0.6	55	28	17	0.24

Appendix C3: List of Soils and their User Codes in the Humbo Watershed

S.No	User Code (Grid Value)	Soil Name (SWAT Code)	Texture Class
1	156	DSOLMap_156	Clay
2	168	DSOLMap_168	Clay
3	301	DSOLMap_301	Silty Clay
4	313	DSOLMap_313	Silty Clay
5	314	DSOLMap_314	Silty Clay
6	317	DSOLMap_317	Silty Clay
7	318	DSOLMap_318	Silty Clay
8	350	DSOLMap_350	Silty Clay
9	361	DSOLMap_361	Silty Clay
10	366	DSOLMap_366	Silty Clay
11	745	DSOLMap_745	Sandy Clay Loam
12	746	DSOLMap_746	Sandy Clay Loam
13	749	DSOLMap_749	Sandy Clay Loam
14	750	DSOLMap_750	Sandy Clay Loam
15	782	DSOLMap_782	Sandy Clay Loam
16	785	DSOLMap_785	Sandy Clay Loam
17	786	DSOLMap_786	Sandy Clay Loam
18	792	DSOLMap_792	Sandy Clay Loam
19	798	DSOLMap_798	Sandy Clay Loam
20	869	DSOLMap_869	Sandy Clay Loam
21	877	DSOLMap_877	Clay Loam
22	889	DSOLMap_889	Clay Loam
23	937	DSOLMap_937	Clay Loam
24	942	DSOLMap_942	Clay Loam
25	1727	DSOLMap_1727	Loamy Sand
26	1728	DSOLMap_1728	Loamy Sand
27	1740	DSOLMap_1740	Loamy Sand
28	1793	DSOLMap_1793	Sandy Loam
29	1800	DSOLMap_1800	Sandy Loam
30	1877	DSOLMap_1877	Sandy Loam
31	1884	DSOLMap_1884	Sandy Loam

Appendix C4: Physicochemical Properties of Soils in the Humbo Watershed

Soil Name	Hyd Grp	Max Depth (mm)	BD (g/cm³)	AWC (mm/mm)	K-sat (mm/hr)	Org Carb (%)	Clay (%)	Silt (%)	Sand (%)	USLE_K
DSOL Map_156	D	2000	1.26	0.149	11.64	3.34	44.3	22.77	32.94	0.12
DSOL Map_168	D	2000	1.22	0.126	18.11	3.04	41.38	18.81	39.56	0.12
DSOL Map_301	D	2000	1.31	0.121	17.33	1.73	40.3	14.06	45.7	0.12
DSOL Map_313	D	2000	1.24	0.128	23.1	1.91	37.72	14.15	48.12	0.11
DSOL Map_314	D	2000	1.3	0.112	23.9	1.66	36.25	13.91	49.88	0.12
DSOL Map_317	D	2000	1.26	0.131	26.75	4.64	30.33	20.86	49.28	0.13
DSOL Map_318	D	2000	1.22	0.124	23.78	2.37	35.16	18.06	46.84	0.12
DSOL Map_350	D	2000	1.24	0.121	26.5	1.94	34.88	15.84	49.47	0.12
DSOL Map_361	D	2000	1.21	0.127	22.36	2.48	36.5	17.53	46.1	0.11
DSOL Map_366	C	2000	1.24	0.138	23.22	3.33	32.5	21.95	46.03	0.12
DSOL Map_745	D	2000	1.24	0.121	26.77	2.31	33.6	16.83	49.47	0.12
DSOL Map_746	D	2000	1.31	0.104	29.31	1.69	33.4	13.54	53.03	0.12
DSOL Map_749	C	2000	1.27	0.119	26.2	4.13	32	18.02	49.94	0.13
DSOL Map_750	C	2000	1.22	0.13	25.14	2.86	33.22	19.28	47.38	0.12
DSOL Map_782	C	2000	1.28	0.112	34.94	2.03	30.36	15.13	54.53	0.12

Soil Name	Hyd Grp	Max Depth (mm)	BD (g/cm³)	AWC (mm/mm)	K-sat (mm/hr)	Org Carb (%)	Clay (%)	Silt (%)	Sand (%)	USLE_K
DSOL Map_785	C	2000	1.32	0.108	45.25	2.23	24.38	17.06	58.56	0.13
DSOL Map_786	C	2000	1.23	0.148	27.73	2.8	29	23.17	47.8	0.13
DSOL Map_792	C	2000	1.29	0.104	45.78	5.17	20.27	20.34	59.53	0.14
DSOL Map_798	C	2000	1.25	0.148	24.2	3.39	30.16	23.83	46.12	0.13
DSOL Map_869	C	2000	1.28	0.112	54.84	2.47	20.03	18.73	61.44	0.14
DSOL Map_877	D	2000	1.21	0.155	15.2	5.99	38.72	24.27	36.9	0.12
DSOL Map_889	D	2000	1.2	0.135	21.39	2.6	36.84	19.58	43.3	0.12
DSOL Map_937	C	2000	1.18	0.157	17.72	3.8	36.56	24.6	38.84	0.12
DSOL Map_942	C	2000	1.21	0.171	18.31	4.63	30.78	31.88	37.34	0.13
DSOL Map_1727	B	2000	1.44	0.037	148.9	0.28	6.36	10.12	83.5	0.11
DSOL Map_1728	B	2000	1.48	0.046	132	0.43	8.63	9.13	82.1	0.11
DSOL Map_1740	B	2000	1.47	0.043	123.7	0.36	8.98	10.31	80.56	0.12
DSOL Map_1793	C	2000	1.39	0.086	65.7	1.57	18.4	15.18	66.3	0.14
DSOL Map_1800	B	2000	1.3	0.109	51.3	5.57	18.72	20.55	60.7	0.14
DSOL Map_1877	B	2000	1.36	0.099	68.44	1.77	16.66	17.08	66.25	0.14

Soil Name	Hyd Grp	Max Depth (mm)	BD (g/cm³)	AWC (mm/mm)	K-sat (mm/hr)	Org Carb (%)	Clay (%)	Silt (%)	Sand (%)	USLE_K
DSOL Map_1884	B	2000	1.18	0.132	70.7	5.62	12.11	25.05	62.84	0.15

Appendix D: SWAT Model Simulation Outputs

Appendix D.1: Monthly Observed vs. Simulated Streamflow (m³/s) for Calibration Period (1990–2000)

Month-Year	Observed Flow (m³/s)	Simulated Flow (m³/s)
Jan-1995	38.56	57.33
Feb-1995	38.22	23.88
Mar-1995	118.10	92.64
Apr-1995	905.61	643.56
May-1995	363.98	390.54
Jun-1995	106.23	141.34
Jul-1995	163.75	237.47
Aug-1995	367.51	336.00
Sep-1995	385.12	532.25
Oct-1995	154.68	217.44
Nov-1995	87.11	98.83
Dec-1995	45.37	32.76
Jan-1996	59.45	82.04
Feb-1996	33.28	94.33
Mar-1996	154.14	172.43
Apr-1996	543.70	457.52
May-1996	588.23	546.27
Jun-1996	371.97	371.97
Jul-1996	287.01	242.42
Aug-1996	352.50	364.51
Sep-1996	368.28	424.48
Oct-1996	198.96	216.82
Nov-1996	117.21	86.22
Dec-1996	43.27	53.45
Jan-1997	44.08	36.23
Feb-1997	25.00	76.76
Mar-1997	81.83	134.32
Apr-1997	403.55	486.18
May-1997	253.59	192.21
Jun-1997	176.52	132.44
Jul-1997	207.86	221.68
Aug-1997	249.05	202.55
Sep-1997	198.18	139.04
Oct-1997	479.70	546.86
Nov-1997	343.24	316.79
Dec-1997	75.00	58.98
Jan-1998	88.281	136.43

Feb-1998	96.914	68.42
Mar-1998	216.651	305.81
Apr-1998	535.21	514.35
May-1998	1038.235	732.16
Jun-1998	253.281	204.85
Jul-1998	300.922	358.49
Aug-1998	525.159	672.65
Sep-1998	534.937	470.89
Oct-1998	610.592	786.56
Nov-1998	164.095	114.69
Dec-1998	50.55	96.07

Appendix D.2: Monthly Observed vs. Simulated Sediment Yield (tons) for Calibration Period

Month-Year	Observed Sediment (tons)	Simulated Sediment (tons)
Jan-1995	1.45	0.44
Feb-1995	0.57	0.03
Mar-1995	24.96	3.14
Apr-1995	4423.5	5962.3
May-1995	443.08	1458.7
Jun-1995	29.98	3.31
Jul-1995	77.1	74.96
Aug-1995	1281.8	1060.9
Sep-1995	792.83	2274.6
Oct-1995	65.71	36.19
Nov-1995	11.45	3.24
Dec-1995	0.78	0.08
Jan-1996	2.95	1.06
Feb-1996	0.36	2.21
Mar-1996	124.95	80.93
Apr-1996	756.96	1945.7
May-1996	1940.0	1894.4
Jun-1996	970.62	668.04
Jul-1996	332.22	237.99
Aug-1996	609.43	1072.5
Sep-1996	561.41	1425.6
Oct-1996	174.52	87.96
Nov-1996	27.35	1.68
Dec-1996	0.55	0.32
Jan-1997	0.57	0.1
Feb-1997	0.07	0.98
Mar-1997	8.69	10.88
Apr-1997	871.26	2158.4
May-1997	186.44	95.59
Jun-1997	64.88	16.59
Jul-1997	115.69	25.86
Aug-1997	194.57	19.78
Sep-1997	124.03	3.29

Oct-1997	1874.6	2700.8
Nov-1997	613.56	642.45
Dec-1997	6.11	0.51
Jan-1998	12.18	10.87
Feb-1998	14.93	0.88
Mar-1998	368.61	243.61
Apr-1998	1441.9	2034.4
May-1998	6263.6	5896.7
Jun-1998	254.89	32.74
Jul-1998	327.99	391.8
Aug-1998	2282.8	4927.9
Sep-1998	1640.2	1752.4
Oct-1998	3227.3	4829.7
Nov-1998	101.99	7.74
Dec-1998	1.21	1.74
Jan-1999	1.16	1.91
Feb-1999	0.47	0.01
Mar-1999	174.05	70.93
Apr-1999	696.53	1395.7
May-1999	138.8	53.86
Jun-1999	6.83	0.88
Jul-1999	173.28	620.4
Aug-1999	1772.3	923.63
Sep-1999	617.2	1797.9
Oct-1999	2384.6	1606.3
Nov-1999	10.51	3.63
Dec-1999	0.44	3.68